Formation mechanisms of molecular compound in saturated-unsaturated mixed-acid triacylglycerols mixture systems and its edible applications

Laura Bayés-García[1] Kiyotaka Sato[2] Lu Zhang[3] Shinichi Yoshikawa[4] Fumitoshi Kaneko[5] Yoshinori Yamamoto[5] Shimpei Watanabe[6] | Ken Taguchi[7]

[1] Departament de Mineralogia, Petrologia i Geologia Aplicada, Facultat de Ciències de la Terra, Universitat de Barcelona, Barcelona, Spain

[2] School of Applied Biological Science, Hiroshima University, Higashi-Hiroshima, Japan

[3] College of Food and Bioengineering, University of Light Industry, Zhengzhou, China

[4] Research Institute for Creating the Future, Fuji Oil Holdings Inc., Izumisano, Japan

[5] Graduate School of Science, Osaka University, Toyonaka, Japan

[6] Research Institute for Creating the Future, Fuji Oil Holdings Inc., Tsukubamirai, Japan

[7] Graduate School of Advanced Science and Engineering, Hiroshima University, Higashi-Hiroshima, Japan

Correspondence: Ken Taguchi, Graduate School of Advanced Science and Engineering, Hiroshima University, Higashi-Hiroshima 739-8521, Japan.

Email: ktaguchi@hiroshima-u.ac.jp

Abstract

The triacylglycerols (TAGs) containing saturated (Sat)-unsaturated (U) fatty acid moieties (S_{at}-U mixed acid TAGs) are widely present in most natural fats and employed in many industrial applications. The mixing behavior of different Sat-U mixed acid TAGs acts important roles in the physicochemical properties TAG-based materials. Among the three main mixing states of miscible, eutectic and molecular compound (MC) forming mixtures, fundamental research has been conducted on the MC crystals formed by different S_{at}-U mixed acid TAGs to understand the structures, phase behavior and crystallization properties. This article reviews studies to date on the complex thermodynamic, kinetic and structural factors that affect the formation of MC crystals in binary and ternary mixtures of Sat-U mixed acid TAGs ($S_{at}US_{at}$, $S_{at}S_{at}U$, $US_{at}U$ and UUS_{at}) through specific molecular interactions among the component TAGs. Furthermore, the application of the MC-forming mixtures containing cacao butter to new types of cocoa butter alternative is reviewed.

1. Introduction

The physicochemical properties (e.g., texture, rheology, melting behavior, spread ability, appearance, etc.) of lipid-based products in the food, pharmaceutical and cosmetic industries are largely determined by the polymorphic and mixing behavior of the constituent triacylglycerols (TAGs) (Floeter et al., 2018; Hartel, 2001; Larsson et al., 2006).

The polymorphic crystallization of TAGs, often based on complex simultaneous processes, and the phase transformation phenomena are determined by many different factors, such as the chemical nature of the fatty acid moieties in the TAG structures, and the crystallization conditions applied, which can be tailored in many different ways by the application of external factors (Bayés-García, Patel, et al., 2015), such as the use of dynamic thermal treatments (Bayés-García et al., 2013; Bayés-García et al., 2016; Bayés-García et al., 2018; Hartel, 2001; Herrera & Hartel, 2000), sonication (Chen et al., 2013; Lee et al., 2015; Martini, 2013; Rincón-Cardona et al., 2015; Ye et al., 2014), shear (Acevedo et al., 2012; Acevedo & Marangoni, 2014; Mazzanti et al., 2011; Sonwai & Mackley, 2006), emulsification (Douaire et al., 2014; Povey, 2014), additives (Bayés-García et al., 2022; Smith et al., 2011; Yoshikawa et al., 2014)). An in-depth understanding of the polymorphism and mixing behavior of TAG components in binary, ternary and even more complex systems is then required for the optimal control and design of industrial lipid crystallization procedures.

The mixing behavior of TAGs has been comprehensively reviewed by several authors (Floeter et al., 2018; Macridachis et al., 2020; Zhang et al., 2018). Among all TAG species, those with saturated-unsaturated mixedacid compositions are widely present in most natural fats and used in industrial applications. Therefore, extensive research has been carried out in their binary (Alishevich et al., 2023; Bayés-García, Calvet, et al., 2015; Cholakova et al., 2023; Ikeda et al., 2010; Ikeda-Naito et al., 2014; Koyano et al., 1992; Minato, Ueno, Smith, et al., 1997; Minato, Ueno, Yano, et al., 1997; Mizobe et al., 2013; Nakanishi et al., 2018; Rousset et al., 1998; Takeuchi et al., 2002; Wijarnprecha et al., 2023; Zhang et al., 2007; Zhang et al., 2009), ternary (Ghazani & Marangoni, 2019a; Koyano et al., 1993; Macridachis et al., 2021; Macridachis et al., 2022; Sasaki et al., 2012; Watanabe et al., 2018; Yoshikawa et al., 2022) and multicomponent mixture systems (Bayés-García et al., 2017; Watanabe et al., 2021). In parallel with the experimental studies on the TAG mixtures, theoretical studies

have been carried out to model and predict the mixing behavior of different TAGs (Seilert et al., 2021; Wesdorp et al., 2013).

Although the number of molecules involved in complex end products is often on the order of several hundred (Gresti et al., 1993; Myher et al., 1988), the study on the solid-state miscibility on a smaller scale with a reduced number of TAG components, usually through binary or ternary mixtures, has been shown to provide highly valuable information that can be extrapolated to real fats, such as extra virgin olive oil (Bayés-García et al., 2017), cocoa butter (Ghazani & Marangoni, 2019a; Ghazani & Marangoni, 2019b; Sasaki et al., 2012), cocoa butter and coconut oil (Joshi et al., 2020), palm oil (Gibon et al., 1986; Gibon & Danthine, 2020; Lu et al., 2019; Minato et al., 1996; Minato, Ueno, Smith, et al., 1997), milk fat/palm oil/palm stearin mixtures (Mao et al., 2023).

There are three main mixed states resulting from molecular interactions in binary systems of TAGs. In a miscible mixture (Figure 1a), a solid solution is formed at all the mixing ratios between the component TAGs with similar thermal stability and a high degree of isopolymorphism, as the integration of one crystal phase into the other does not cause any significant disturbance in crystal packing (Lusi, 2018). By contrast, dissimilar TAG components lead to eutectic behavior as shown in Figure 1b, where the eutectic composition and the degree of partial solid miscibility can be determined by, among other things, chain-length structures and melting behavior (Cholakova et al., 2023; Floeter et al., 2018; Minato et al., 1996; Timms, 1984).

Of particular interest is the third mixed state of the molecular compound (MC) formation (Figure 1c). This stoichiometric compound is formed only at well-defined compositions by specific molecular interactions between individual TAGs, resulting in unique structural and thermodynamic properties (see below). Molecular compounds in TAG systems are usually formed by TAG components at equal quantities (1:1 ratio) in a well-defined arrangement within the crystal lattice. The wide range of possibilities given by chemical nature and processing conditions of the component TAGs may be further enhanced by the use of MC products due to their applicability in edible fat structuring. For example, the potential of MC crystals as partial replacers for trans or saturated fats has already been demonstrated by increasing melting temperature, hardness and solid fat content (Mykhaylyk et al., 2007).

In this review, a special emphasis has been given to the crucial role and potential applicability of MC-forming mixture systems to modify of the physicochemical properties of lipid structures. It should be noted that complex thermodynamic, kinetic and structural factors largely affect the formation of MC in saturated-unsaturated-saturated ($S_{at}US_{at}$)/$US_{at}U$ and $S_{at}US_{at}$/S_{at}-$S_{at}U$ systems through specific molecular interactions among the component TAGs.

As a fundamental study to elucidate the formation mechanisms of MC, precise observation was performed on the crystallization behavior of palmiticoleic-based MC of 1,3-dipalmitoyl-2-oleoyl-glycerol (POP)/1,3-dioleoyl-2-palmitoyl glycerol (OPO), POP/1,2-dipalmitoyl-3-oleoyl-rac-glycerol (rac-PPO) and POP/1,2-dipalmitoyl-3-oleoyl-sn-glycerol (sn-PPO) when subjected to varied cooling rates. By comparing the crystallization behavior of POP/sn-PPO and POP/rac-PPO systems, the effects of glycerol structures and optical isomerization on MC crystal formation were also briefly described (Bayés-García et al., 2023). The analysis of the influence of the cis-trans isomerization on MC formation was performed by replacing cis-oleoyl to transelaidoyl (E) chains in the binary system of 1,3-dipalmitoyl-2-elaidoyl glycerol (PEP)/1,3-dielaidoyl-2-palmitoyl glycerol (EPE) (Zhang et al., 2020).

The effects of MCs as polymorphic stabilizers of a third TAG component were discovered by Yoshikawa et al., who observed the crystallization kinetics in ternary mixtures of 1,3-distearoyl-2-oleoyl glycerol (SOS)/1,3-dioleoyl-2-stearoyl glycerol (OSO)/1,2,3-trilauroyl glycerol (LLL) (Yoshikawa et al., 2022). It was found that the β-crystals of $MC_{SOS/OSO}$ triggered crystallization of the most stable β-form of LLL. This indicates the possibility to develop a novel cocoa butter substitute (CBS) through the incorporation of TAGs which forms β-2 crystals of MC and thereby promotes β-2 crystallization of lauric fats. As a result, the possibility of fat blooming caused by the transformation of lauric fat crystals from β'-2 to β-2 can be reduced.

Until recently, the application of MC formation to the end food products has been rather limited (Sibbald et al., 2016). However, systematic work was carried out to apply the MC-forming mixtures to the development of cocoa butter equivalent (CBE) and CBS formulations by forming the MC crystals in the ternary mixtures of cocoa butter, OSO, SSO and LLL fats (Watanabe et al., 2021; Watanabe et al., 2023). These studies may have

138 indicated the high potential of the MC-forming TAG mixtures to produce the edible fats with
139 novel functionality

140

MOLECULAR-LEVEL UNDERSTANDING OF THE FORMATION MECHANISMS OF MC CRYSTALS

Here briefly summarized are the main results of previous studies on the formation processes, structural properties and phase behavior of MC crystals.

It has been found that the following TAGs can form the MC crystals in their binary mixtures, in which the ratio of the component TAGs is always 50:50.

$S_{at}US_{at}$: Symmetric saturated and unsaturated TAGs such as POP, SOS, PEP

$S_{at}S_{at}U$: asymmetric saturated and unsaturated TAGs such as PPO (or OPP), SSO

$US_{at}U$: symmetric unsaturated and saturated TAGs such as OPO, OSO, EPE

UUSat: asymmetric unsaturated and saturated TAGs such as OOS (or SOO) and OOP (or POO)

Figure 2 illustrates the combination of the TAGs, noting the MC-forming and eutectic mixtures. In the binary mixtures of $S_{at}US_{at}/S_{at}S_{at}U$ and $S_{at}US_{at}/US_{at}U$, the MC crystals are formed in the metastable α, β' and β polymorphs, as confirmed in the mixtures of SOS/OSO (Engström, 1992; Koyano et al., 1992), SOS/SSO (Takeuchi et al., 2002), POP/OPO (Minato, Ueno, Yano, et al., 1997; Minato et al., 1997), POP/PPO (Minato, Ueno, Smith, et al., 1997; Minato et al., 1997), PEP/EPE (Zhang et al., 2020). However, the MC crystals are not formed and fully eutectic mixtures are formed in the combinations of $S_{at}US_{at}/UUS_{at}$ and $S_{at}S_{at}U/US_{at}U$. The former result was confirmed in the mixtures of POP/OOP (Zhang et al., 2007) and SOS/OOS (Zhang et al., 2009), and the latter result was confirmed in the mixture of PPO/OPO (Bayés-García, Calvet, et al., 2015).

Interestingly, the MC crystals were formed in the mixtures of $US_{at}U/UUS_{at}$ and $S_{at}S_{at}U/UUS_{at}$ in their metastable states. For example, the MC crystals in the OPO/OOP and PPO/OOP mixtures occurred only under metastable conditions and tended to separate into component TAGs to form eutectic mixture systems after 17 months of storage (Bayés-García, Calvet, et al., 2015). These results were in contrast to those of previous studies on $S_{at}US_{at}/S_{at}S_{at}U$ and $S_{at}US_{at}/US_{at}U$ in which the MC crystals are thermodynamically stable (Minato, Ueno, Smith, et al., 1997; Minato, Ueno, Yano, et al., 1997).

169 The molecular understanding of the ability and inability to form the MC crystals is still
170 open to question. The main key factors may be the stabilization of chain packing between
171 unsaturated and saturated chains, π–π interactions between the double bonds in the
172 unsaturated chains and stabilization of glycerol conformations.

173 Figure 3 illustrates the glycerol conformations and structural models of the MC
174 crystals by taking palmitic and oleic chains as Sat and U chains, respectively. The glycerol
175 conformations are tuning fork in POP and OPO, and chair in PPO and OOP, and all the
176 TAGs form triple chain length in their stable polymorphic forms of β-3 in POP and OPO,
177 and β'-3 in PPO and OOP (Bayés-García, Calvet, et al., 2015; Floeter et al., 2018). Three
178 problems may arise in the formation of the MC crystals of the double chain- length structure:
179 the chain packing between palmitic and oleic chains, stacking of glycerol groups between
180 the tuning fork and chair conformations, and the π–π interactions between the unsaturated
181 chains.

182 In the case of $MC_{POP/OPO}$, the stacking of the glycerol groups may be easily
183 accomplished, since both component TAGs form the tuning fork conformation. The chain-
184 chain packing including the π–π interactions may be easiest in $MC_{POP/OPO}$, and thus the
185 formation of $MC_{POP/OPO}$ can be easily done.

186 However, the stacking of the glycerol groups in $MC_{POP/PPO}$ may be difficult since
187 POP and PPO exhibit the tuning fork and chair conformations, respectively. In addition,
188 steric hindrance between the oleic and palmitic chains may be a disturbing factor in the
189 formation of $MC_{POP/PPO}$. Nevertheless, the metastable and stable polymorphs are formed
190 in $MC_{POP/PPO}$. This suggests that the strong attractive interactions between palmitic chains
191 may play dominant roles during the formation processes of $M_{CPOP/PPO}$.

192 In the case of $MC_{OPO/OOP}$, the stacking of the tuning fork (OPO) and chair (OOP)
193 glycerol conformations may not be easy, and the chain packing between the palmitic and
194 oleic chains is rather unstable. Therefore, $MC_{OPO/OOP}$ is not thermodynamically stable. In
195 the case of PPO/OOP, it seems that both the chain packing and the stacking of the chair
196 glycerol conformation of PPO and OOP may enable the formation of MC crystals, but
197 $MC_{PPO/OOP}$ is not thermodynamically stable. Finally, the structures of $MC_{POP/OOP}$ and

198 $MC_{PPO/OPO}$ are unstable because the stacking of the glycerol groups and the chain packing
199 may not stabilize the MC crystals. To conclude, the explanation of the formation of MC
200 crystals at the molecular level seems to be incomplete except for $MC_{POP/OPO}$ and
201 $MC_{POP/PPO}$, and further research is needed.

202 The crystallization kinetics of MC depends on the TAG molecular structures as well
203 as the rate of cooling. For example, quite rapid cooling (>40°C/min) of the binary mixture
204 of POP/OPO resulted in separate crystallization of POP and OPO in the first, while
205 $MC_{POP/OPO}$ crystals started to form in addition to the POP and OPO crystals with
206 decreasing cooling rates (<30°C/min). The extent of the MC_{POP}/OPO crystals increased
207 with decreasing cooling and heating rates after crystallization (Nakanishi et al., 2018). This
208 result indicates that the formation of MC is a kinetic process involving competitive
209 crystallization and structural rearrangement of the component TAGs.

210 Another interesting issue is the effect of racemization and optical isomerization of
211 asymmetric $S_{at}S_{at}U$ and UUS_{at} on the formation of MC when mixed with other TAGs. For
212 example, the phase behavior of POP/rac-PPO and OPO/sn-PPO is somewhat different in
213 terms of the melting points of $MC_{POP/rac\text{-}PPO}$ and $MC_{OPO/sn\text{-}PPO}$, although both mixtures
214 form stable polymorph of the double chain length structure (β-2). This may be related to the
215 different crystallization kinetics of $MC_{POP/rac\text{-}PPO}$ and $MC_{POP/sn\text{-}PPO}$ (see below).

216

217

218

FORMATION OF MC IN BINARY MIXTURES OF PEP/EPE

Replacing the cis oleoyl chain in a TAG with a trans isomeric elaidoyl chain drastically changes its physical and even nutritional properties. However, very little is known about the actual crystal structures and phase behavior of elaidoyl-containing TAGs. To clarify the effect of cis-trans isomerization on the crystallization behavior of TAGs, the phase behavior of binary mixtures of 1,3-dipalmitoyl-2-elaidoyl-glycerol (PEP) and 1,3-dielaidoyl-2-palmitoyl-glycerol (EPE) was investigated (Zhang et al., 2020). The binary mixtures of PEP and EPE were prepared at 10% intervals and characterized by DSC, conventional powder X-ray diffraction, and synchrotron radiation x-ray diffraction (SR-XRD). The effects of cis-trans isomerization on the crystallization behavior of TAGs were examined by comparison with related cis and fully saturated counterparts.

The most stable polymorphic forms are β' for PEP, but β for EPE (Zhang et al., 2020). The formation of MC crystals was first observed in the PEP/EPE mixture at a 50:50 ratio, as shown in the phase diagram (Figure 4). The PEP-rich region exhibited a monotectic phase for β-form MC and β'-form PEP, whereas the EPE-rich region exhibited a monotectic phase for β-form MC and β-form EPE, which is quite similar to that observed for the POP/OPO (Minato, Ueno, Yano, et al., 1997).

The temperature dependence of the SR-XRD patterns and the DSC thermogram of PEP/EPE at a 50:50 ratio taken during cooling and heating at a rate of 2°C/min is shown in Figure 5. The simultaneous crystallization of the β' form of $MC_{PEP/EPE}$ along with the α form was confirmed in the WAXS spectra by the appearance of β' peaks of 0.44 and 0.39 nm and an α peak of 0.42 nm, as indicated by the arrows. With increasing temperature, the α form transformed into the β' form and then further transformed to the thermodynamically stable β form via solid-state transformation. Then, the β form of MC melted at approximately 48°C. In the SAXS spectra, the solid-state transition of $\alpha \rightarrow \beta' \rightarrow \beta$ was confirmed by the shifting of the peak from 4.62 to 4.32 nm and then to 4.25 nm.

Figure 6 shows the structural model of $MC_{PEP/EPE}$ using the tuning fork conformation of glycerol group, which allows the void (see arrow) at the methyl end of PEP in β' form due to the chain length mismatch between neighboring P and E chains to be filled by the acyl chain of EPE, as indicated by the dotted line. It is worth noting that when the "O" in certain binary mixtures of palmitic-oleic diacid TAGs such as POP and POO was replaced

with “S,” or even “E,” the phase behavior remained the same. For example, a eutectic phase was found in both the POP/POO (Zhang et al., 2007) and PSP/rac-PSS mixtures (Bhaggan et al., 2018), and the MC-forming mixture was formed in the POP/rac-PPO (Minato, Ueno, Smith, et al., 1997) and PSP/rac-PPS mixtures (Boodhoo et al., 2009). The MC-forming mixture was also found in the POP/OPO (Minato, Ueno, Yano, et al., 1997) and PEP/EPE mixtures (Zhang et al., 2020), and thus it is speculated that MC is formed in the PSP/SPS mixture.

CRYSTALLIZATION KINETICS OF MC CRYSTALS OF POP/OPO AND POP/PPO

To elucidate the effects of glycerol structures on the kinetic properties of MC-forming mixture phases, thermal analysis, x-ray diffraction and optical microscopy techniques were applied to the binary mixtures of POP/OPO, POP/rac-PPO and POP/1,2-dipalmitoyl-3-oleoyl-sn-glycerol (sn-PPO) (Bayés-García et al., 2023). All the three mixtures exhibited the MC-forming mixture at a 1:1 ratio.

The mixture samples were subjected to dynamic conditions of cooling at low and intermediate rates of 0.1, 0.5, and 2°C/min to complete crystallization and reheating at a constant rate of 2°C/min, while monitoring complex crystallization and polymorphic transition phenomena, as summarized in Figure 7. The POP/OPOmixture formed only $MC_{POP/OPO}$ crystals with double chainlength structure in its most stable β form when cooled under all the conditions analyzed, and they simply melted when heated. The occurrence of $MC_{POP/OPO}$ β form was reported in both pure liquid (Minato, Ueno, Yano, et al., 1997) and n-dodecane solution systems (Ikeda et al., 2010).

Similarly, the most stable β form of $MC_{POP/rac\text{-}PPO}$ crystallized when cooled at 0.1°C/min, although a metastable β' form was detected at 0.5 and 2°C/min, which transformed to β when heated. By contrast, the POP/sn-PPO mixture showed significantly complex polymorphic events in all the experimental conditions studied, showing the coexistence of $MC_{POP/sn\text{-}PPO}$ with polymorphs of pure POP and sn-PPO component TAGs, even at the lowest cooling rate applied. In more detail, the 1:1 TAGs mixture crystallized into β' forms of sn-PPO (triple chain length), $MC_{POP/sn\text{-}PPO}$ (double chain length) and POP (double chain length) at 0.1 and 0.5°C/min. When heated, the metastable β' of $MC_{POP/sn\text{-}PPO}$ transformed into its most stable β form before melting. At a higher cooling rate of 2°C/min, the least stable polymorphs predominated, showing complicated simultaneous crystallization processes of sn-PPO β' form (triple chain length) and α forms (double chain length) of $MC_{POP/sn\text{-}PPO}$, POP and sn-PPO. Subsequent heating caused polymorphic transformations of $\alpha \rightarrow \beta' \rightarrow \beta$ for MCPOP/sn-PPO, and $\alpha \rightarrow L \rightarrow \beta'$ for POP (see Figure 7).

Regarding the effects of optical isomerization in mixed systems of TAGs, extensive work had previously been carried out by Craven and Lencki (2013). Additionally, Mizobe et al. analyzed the polymorphic structures of R-PPO, S-OPP and their mixtures, and concluded that the two optical isomers had identical structural properties, whereas the polymorphic characteristics of R-PPO and rac-PPO became different, with the latter corresponding to the 1:1 mixture of R-PPO/S-OPP (Mizobe et al., 2013).

To understand the differences in the crystallization behavior of $MC_{POP/OPO}$ and $MC_{POP/sn\text{-}OPO}$, one can pay attention to their structural models, which are mainly based on the glycerol structures of POP, OPO and sn-PPO, as depicted in Figure 8 (Bayés-García et al., 2023). It can be assumed that the tuning fork glycerol conformation is the most stable one for both POP and OPO β forms, since the palmitic and oleic acid chains are located on different leaflets, favoring the packing of TAG molecules in triple chain-length structures that avoid the steric hindrance between straight palmitic and bent oleic acid chains. By contrast, the sn-PPO β' form may exhibit a chair-type glycerol conformation, which is also packed in a triple chain-length structure for the same reasons explained above.

During the formation process of the MC crystals, the chain-length structures were changed from triple to double, and close packing of glycerol groups and palmitic and oleic acid chains of neighboring TAG molecules occurred. A higher ability of $MC_{POP/OPO}$ to form and stabilize in β form compared to other MCs was observed, since the tuning fork-type glycerol conformation of the two TAG components POP and OPO can be maintained in $MC_{POP/OPO}$, resulting in a β-2 structure with palmitic and oleic acid chains packed in separate leaflets. This ability was not observed in the POP/sn-PPO mixture, as it did not form $MC_{POP/sn\text{-}PPO}$ alone, but it coexisted with single POP and sn-PPO TAG components. Polarized light microscopy data confirmed a higher crystallization rate for sn-PPO crystals compared to other single TAGs or MCs, which may explain the separate crystallization when the POP/sn-PPO mixture was cooled, and this may also be explained from a structural point of view (Bayés-García et al., 2023). According to the described model (Figure 8), an extra molecular rearrangement may occur during the $MC_{POP/sn\text{-}PPO}$ formation, based on the change of the chair-type glycerol conformation of sn-PPO to the tuning fork-type, leading to an MC with coexisting oleic and palmitic acid chains in the same leaflet.

Regarding the different crystallization behavior of $MC_{POP/sn\text{-}PPO}$ and $MC_{POP/rac\text{-}PPO}$, one may consider the ability of R-PPO and S-OPP to form a stable molecular packing (or racemic compound), which may interact with POP molecules to form a stable MC structure.

However, further work may be required to understand the mechanisms involved.

INTERACTIVE POLYMORPHIC CRYSTALLIZATION OF MCSOS/OSO AND LLL

The effect of MC formation on the polymorphic crystallization of the other coexisting TAG was examined using ternary TAG mixtures of LLL/SOS/OSO with a 1:1 weight ratio of SOS and OSO (SOS/OSO = 1/1) (Yoshikawa et al., 2022).

Under a series of thermal conditions of cooling from the melt, isothermal holding, and heating, pure LLL without containing SOS and OSO formed β' form crystals, which transformed to β form during the heating process after the crystallization. In 1992, it was found that the binary TAG mixture of SOS/OSO =1/1 formed mainly β-form MC crystals of SOS and OSO ($MC_{SOS/OSO}$) during the cooling process (Koyano et al., 1992). Based on these results, the ternary mixtures of LLL/SOS/OSO/ at various mixing ratios of LLL and SOS/OSO = 1/1 were investigated and the immiscible eutectic behavior was observed with retarded crystallization and lowered melting points of the formed crystals (Figure 9). Quite interesting results were found in the crystallization kinetics of two β forms of $MC_{SOS/OSO}$ and LLL; the β crystallization of $MC_{SOS/OSO}$ coincided with the β' to β transformation or direct β meltcrystallization of LLL during the isothermal-holding process, as evident from the synchrotron radiation x-ray diffraction (SR-XRD) data shown in Figure 10. This coincidence strongly suggests the possibility that β crystallization of $MC_{SOS/OSO}$ triggered the β crystallization of LLL. As a result, the spherulitic crystals of LLL deformed and changed their size distribution with increasing concentration of SOS/OSO = 1/1. These peculiar phenomena of the interrelationships between the crystallization of β forms of $MC_{SOS/OSO}$ and LLL have been defined as "interactive polymorphic crystallization" (Yoshikawa et al., 2022).

As a possible mechanism underlying the interactive polymorphic crystallization, epitaxial effects through triclinic-parallel ($T_{//}$) subcell matching between β crystals of LLL and $MC_{SOS/OSO}$ may occur in the same manner that β' form seed crystals of tripalmitin or tristearin effectively accelerated β' crystallization of coconut oil through orthorhombic-perpendicular (O_2) subcell matching (Mahisanunt et al., 2021). Another possible mechanism is martensitic transformation via cooperative displacement of atoms without diffusion in the

crystal lattices, which can be initiated by the occurrence of local stress through mechanical or thermal stimulation, as indicated for petroselinic acid (Kaneko et al., 1997).

Elucidating the mechanism of interactive polymorphic crystallization requires further research, such as SR-XRD experiments substituting the component TAGs (LLL, SOS, and OSO) with the other corresponding TAGs (e.g., SSS, SSO, and SOO, respectively) and SR-XRD experiments using a microbeam technique to analyze the local orientation of TAG molecules near the crystal-crystal interfaces. For example, the SR-XRD data shown in Figure 11 indicate that the effect of facilitating β crystallization of LLL in LLL/SOS/OSO was weakened by replacing OSO with rac-SOO, probably because SOS and SOO crystallized separately in the less stable forms of SOS 5L (2L + 3L), in which SOS formed in randomly packed double and triple chain-length structures (Mykhaylyk et al., 2007), and SOO β'.

It may be worth noting that the study of LLL/SOS/OSO mixtures can be applied to solve the problem of fat blooming in CBS-based compound coatings, which is partly caused by the polymorphic transformation of lauric acidbased TAG crystals in CBS from β'-2 to β-2 (see below).

APPLICATION OF MC CRYSTALS TO NEW TYPES OF COCOA BUTTER EQUIVALENT (CBE) AND COCOA BUTTER SUBSTITUTE (CBS)

Cocoa butter (CB) is indispensable ingredient in chocolate, as it is responsible for the physical properties such as hardness, texture, and melting behavior of chocolate products (Talbot, 2017). However, CB is one of the most expensive ingredients of chocolate and its price is gradually increasing due to several global issues such as low productivity of cacao due to climate change and increasing demand for cacao products (Afoakwa, 2016). Therefore, the confectionery industry has developed CB alternative fats (CBAs) with various functionalities to replace or blended with CB in chocolate production.

CBAs can be classified into three groups based on their compositions: cocoa butter equivalent (CBE), cocoa butter replacer (CBR) and cocoa butter substitute (CBS) (Timms, 2003). Recently, two experimental studies on the physical properties and fat bloom stability of chocolate made with $S_{at}S_{at}U$ and $US_{at}U$ type fats forming MC crystals with CB revealed that these fats can be used as new types of CBA fats (Watanabe et al., 2021; Watanabe et al., 2023).

CBE

Systematic studies showed that the ternary mixtures of SOS, rac-SSO and OSO form MC crystals of stable β-2 form at a concentration of SOS of 50% with different concentrations of SSO and OSO (Watanabe et al., 2018). Figure 12 shows that the MC crystals with the stable β-2 polymorph are formed in a series of the ternary mixtures of SOS/SSO/OSO, in which the ratio of SOS/(SSO + OSO) was set to 50/50 and the ratio of SSO/OSO was varied. Interestingly, it was also observed that stable β-2 of ternary mixtures of SOS/SSO/OSO were formed during simple cooling and heating process after the transformation from the metastable formed to stable form of $MC_{SOS/SSO}$ (Watanabe et al., 2018). These results indicated the formation of new type of CBE which can form a stable β-2 structure in a simple cooling process that can be applied to confectionery products. Based on this study, it was expected that the ternary mixtures can produce a new type of CBE with the stable polymorphic structure when SOS, SSO, and OSO are replaced with CB, SSO-fat and OSO-fat. The SSO-fat and OSO-fat were prepared by full-hydrogenation, interesterification, and fractionation of canola oil high oleic sunflower oil (Watanabe et al., 2021). The physical properties and fat bloom stability of chocolates containing SSO-fat and OSO-fats, which were solidified by simple cooling without tempering process, were then evaluated (Watanabe et al., 2021). Stable β-2 form was observed in the ternary fat mixture of CB/SSO-fat/OSO-fat = 50/20/30–50/3/47 without any tempering processes. Furthermore, chocolate sample containing these fat mixtures did not show fat bloom for 1 year storage test at any storage conditions.

It should be noted that in the chocolate fat phases, the final ratio of the three types of TAG, $S_{at}US_{at}/S_{at}$-$S_{at}U/US_{at}U$, were 50/50/0–50/0/50. Figure 13 shows the temperature change in solid fat content (SFC) values of six fat blends and CB, where the concentrations (%) of $S_{at}US_{at}/S_{at}S_{at}U/US_{at}U$ in the fat blends are 50/46/4 (sample A), 50/40/10 (B), 50/30/20 (C), 50/20/30 (D), 50/10/40 (E), and 50/3/47 (F). The SFC measurement of ternary fat blends of CB, SSO-fat and OSO-fat showed sharp melting profiles around body temperature. Similarly, in the hardness measurement chocolate samples prepared with fat blends of $S_{at}US_{at}/S_{at}S_{at}U/US_{at}U$ = 50/30/20–50/20/30 showed almost the same hardness as that of pure chocolate (Watanabe et al., 2021). In addition, no fat bloom formation was observed in dark chocolate with the fat blends of $S_{at}US_{at}/S_{at}S_{at}U/US_{at}U$ of 50/20/30–

50/0/50 during the one-year storage under isothermal condition at 25°C and thermal cycling condition between 20 and 30°C. Overall, the CB, SSO-fat, and OSO-fat blends can be used as a cocoa butter equivalent (CBE) without tempering procedures (Watanabe et al., 2021).

CBS

The MC crystals made of CB and OSO-fat ($MC_{CB/OSO}$) were applied to compound chocolate formulations by blending with lauric cocoa butter substitutes (CBS) (Watanabe et al., 2023). Conventional CBSs have been produced by fractionation, hydrogenation and a combination of these processes of lauric fats derived from palm kernel oil and other natural fats (Rossell, 1985). These fats are composed of TAGs with lauric (L) and myristic (M) acid moieties including LLL, LLM, LMM, and MMM which are crystallized into β'-2 form by simple cooling without tempering (Smith, 2012). However, the CBS-based chocolate can potentially convert from the β'-2 to β-2 form, which leads to fat bloom formation during long-term storage, because mono-acid TAGs such as LLL and MMM have the potential to transform from β'-2 to the more stable β-2 form (β-tending; Koizumi et al., 2022). In addition, cacao solids such as cacao powder and cacao liquor are often blended to improve the flavor and taste of compound chocolate, resulting in more serious fat bloom due to the phase separation of CBS and CB followed by polymorphic transformation of CB TAGs. This eutectic effect makes it difficult to blend more than 5% cocoa butter in the compound chocolates (Laustsen, 1991).

As described in the previous section, studies on the polymorphic crystallization behavior of the ternary mixture system of LLL/SOS/OSO with the SOS/OSO ratio of 1/1 have revealed that the crystallization of β-2 form in $MC_{SOS/OSO}$ promoted the crystallization and polymorphic transformation of β'-2 to β-2 in LLL (Yoshikawa et al., 2022). Based on these results, the physical properties and fat bloom stability of lauric-based compound chocolate with $MC_{CB/OSO}$ were evaluated (Watanabe et al., 2023).

Table 1 shows six chocolate samples with the different relative concentrations (%) of CBS, OSO-fat and CB investigated. The SFC studies showed that the fat blends of CBS and $MC_{CB/OSO}$ exhibited immiscible eutectic behavior, as did the fat blends of CBS and CB. The results of SFC value, crystallization rates and hardness of compound chocolate with $MC_{CB/OSO}$ suggested that the compound chocolate is suitable for the chocolate production up to about 20% of $MC_{CB/OSO}$ in the fat phases (Watanabe et al., 2023).

In the fat bloom evaluation studies, while CBS/CB compound chocolate, A1-A4, exhibited severe fat bloom within a few weeks, the CBS/CB/OSO-fat compound chocolate,

B1-B4, showed no fat bloom under any storage condition for 6 months (Table 2). In addition, the XRD studies revealed that no polymorphic transformation occurred for the CBS/CB/OSO-fat blends in group B during the 6 months storage, while the polymorphic transformation from β'-2 to β-2 was observed for the fat blends of CBS/CB in group A (Figure 14). The polymorphic transformations of CB TAGs and β-tending TAG in CBS cause fat blooming in CBS-based compound chocolate. Therefore, the mechanisms of fat blooming inhibition in compound chocolate made of CBS/CB/OSO-fat summarized in Table 1 can be assumed that β-tending TAG fractions in the CBS, such as LLL and MMM, may crystallize into β-form during the cooling process via interactive polymorphic crystallization with MCCB/OSO. However, further studies are required to elucidate these mechanisms.

CONCLUSION

The study of the mixing behavior of principal TAGs and various natural and industrialized fats is of great importance, as it is one of the most informative and applicable studies to improve the physicochemical properties of lipid-based products using natural and technologically-produced lipid materials. Until recently, the phases of MC-forming mixture have been studied from a fundamental point of view using pure samples of saturated-unsaturated mixed-acid TAGs. However, the fat materials produced by full-hydrogenation, interesterification, and fractionation of vegetable fats and oils have been used for the application of the MC crystals to end products such as fat spreads and confectionery fats. The physical properties of the MC crystals are different from those of the component TAGs and can improve the end products when applied; for example, the formation of MC crystals containing the mixed acid TAGs with oleic acid moiety can reduce the use of saturated fats (Sibbald et al., 2016), and the application of the MC crystals containing CB, OSO-fat, and SSO-fat to CBE and CBS improved the crystallization kinetics and fat bloom stability. It is expected to explore the molecular mechanisms of the ability and inability of MC formation, and the application of the MC crystals to other end products such as emulsified and aerated systems.

Author contributions

Laura Bayés-García, Ken Taguchi, Lu Zhang, Shinichi Yoshikawa, Fumitoshi Kaneko, Yoshinori Yamamoto, and Shimpei Watanabe performed the experiments and published their original articles, which are reviewed in this article. Kiyotaka Sato initiated and organized this work.

Funding information

Ministerio de Ciencia e Innovación, Grant/Award Number: PID2019-107032RBI00; National Natural Science Foundation of China, Grant/Award Number: 31401661; Generalitat de Catalunya, Grant/Award Number: 2021 SGR 00262; MCIN/AEI/10.13039/501100011033/

Conflicts of Interest

The authors declare that they have no conflict of interest.

Acknowledgements

The acknowledgment is given to the National Natural Science Foundation of China (Grant No. 31401661) and the Photon Factory Program Advisory Committee (Proposal No. 2017G648 & 2018G092), whose support enabled to perform the experiments shown in Figures 4 and 5. The acknowledgment is also given to the Photon Factory Program Advisory Committee (Proposal No. 2019G065 and 2021G049), whose support enabled us to perform the experiments shown in Figures 10 and 11. The study on MC crystals of POP/OPO and POP/PPO (Figures 7 and 8) was supported by the Generalitat de Catalunya through project 2021 SGR 00262, and Grant PID2019-107032RBI00 funded by MCIN/AEI/10.13039/501100011033/.

ORCID

Laura Bayés-García https://orcid.org/0000-0003-1481-581X

Lu Zhang https://orcid.org/0000-0002-8902-0520

Shinichi Yoshikawa https://orcid.org/0000-0003-1224-8743

Fumitoshi Kaneko https://orcid.org/0000-0001-8254-2265

Shimpei Watanabe https://orcid.org/0000-0002-9040-3887

Ken Taguchi https://orcid.org/0000-0003-1276-0499

References

(1) Acevedo NC, Block JM, Marangoni AG. Unsaturated emulsifier mediated modification of the mechanical strength and oil binding capacity of a model edible fat crystallized under shear. Langmuir. 2012;28:16207–17. https://doi.org/10.1021/la303365d

(2) Acevedo NC, Marangoni AG. Functionalization of noninteresterified mixtures of fully hydrogenated fats using shear processing. Food Bioproc Technol. 2014;7:575–87. https://doi.org/10.1007/s11947-013-1110-z

(3) Afoakwa EO. World cocoa production, processing and chocolate consumption pattern. In: Afoakwa EO, editor. Chocolate science and technology. West Sussex, UK: Wiley & Blackwell; 2016. p. 17–48.

(4) Alishevich K, Berˇcíkova M, Kyselka J, Sasínova K, Honzíkova T, Sˇ imicova P, et al. Binary phase behavior of 2-oleoyl-1-palmitoyl-3-stearoyl-rac-glycerol (POS) and 2-linoleoyl-1-palmitoyl-3-stearoyl-rac-glycerol (PLS). Food Biophys. 2023;18:161–73. https://doi-org.sire.ub.edu/10.1007/s11483-022-09761-8

(5) Bayés-García L, Calvet T, Cuevas-Diarte MA. Effects of dynamic temperature variations on microstructure and polymorphic behavior of lipid systems. In: Sato K, editor. Crystallization of lipids. Fundamentals and applications in food, cosmetics and pharmaceuticals. Hoboken, NJ, USA: Wiley-Blackwell; 2018. p. 183–210. https://doi.org/10.1002/9781118593882.ch6

(6) Bayés-García L, Calvet T, Cuevas-Diarte MA, Ueno S. In situ crystallization and transformation kinetics of polymorphic forms of saturated-unsaturated-unsaturated triacylglycerols: 1-palmitoyl-2,3-dioleoyl glycerol, 1-stearoyl-2,3-dioleoyl glycerol, and 1-palmitoyl-2-oleoyl-3-linoleoyl glycerol. Food Res Int. 2016;85: 244–58. https://doi.org/10.1016/j.foodres.2016.05.011

(7) Bayés-García L, Calvet T, Cuevas-Diarte MA, Ueno S. From Trioleoyl glycerol to extra virgin olive oil through multicomponent triacylglycerol mixtures: crystallization and polymorphic transformation examined with differential scanning calorimetry and X-ray diffraction techniques. Food Res Int. 2017;99:476–84. https://doi.org/10.1016/j.foodres.2017.06.015

(8) Bayés-García L, Calvet T, Cuevas-Diarte MA, Ueno S, Sato K. Crystallization and transformation of polymorphic forms of trioleoyl glycerol and 1,2-dioleoyl-3-rac-linoleoyl glycerol. J Phys Chem B. 2013;117:9170–81. https://doi.org/10.1021/jp403872a

(9) Bayés-García L, Calvet T, Cuevas-Diarte MA, Ueno S, Sato K. Phase behavior of binary mixture systems of saturated-unsaturated mixed-acid triacylglycerols: effects of glycerol structures and chain-chain interactions. J Phys Chem B. 2015;119:4417–27.

591 https://doi.org/10.1021/acs.jpcb.5b00673

592 (10) Bayés-García L, Fukao K, Konishi T, Sato K, Taguchi K. Crystallization and transformation
593 behavior of triacylglycerol binary mixtures forming molecular compounds of POP/OPO,
594 POP/rac-PPO, and POP/sn-PPO. Cryst Growth Des. 2023;23: 2870–81.
595 https://doi.org/10.1021/acs.cgd.3c00038

596 (11) Bayés-García L, Patel AR, Dewettinck K, Rousseau D, Sato K, Ueno S. Lipid crystallization
597 kinetics – roles of external factors influencing functionality of end products. Curr Opin Food
598 Sci. 2015;4:32–8. https://doi.org/10.1016/j.cofs.2015.04.005

599 (12) Bayés-García L, Yoshikawa S, Aguilar-Jiménez M, Ishibashi C, Ueno S, Calvet T.
600 Heterogeneous nucleation effects of talc particles on polymorphic crystallization of cocoa
601 butter. Cryst Growth Des. 2022;22:213–27. https://doi.org/10.1021/acs.cgd. 1c00859

602 (13) Bhaggan K, Smith KW, Blecker C, Danthine S. Polymorphism and kinetic behavior of binary
603 mixtures of trisaturated triacylglycerols containing palmitic and stearic acid under non-
604 isothermal conditions. Eur J Lipid Sci Technol. 2018;120:1800072.
605 https://doi.org/10.1002/ejlt.201800072

606 (14) Boodhoo MV, Bouzidi L, Narine SS. The binary phase behavior of 1, 3-dipalmitoyl-2-
607 stearoyl-sn-glycerol and 1, 2-dipalmitoyl-3-stearoyl-sn-glycerol. Chem Phys Lipids.
608 2009;160:11–32. https://doi.org/10.1016/j.chemphyslip

609 (15) Chen F, Zhang H, Sun X, Wang X, Xu X. Effects of ultrasonic parameters on the
610 crystallization behavior of palm oil. J Am Oil Chem Soc. 2013;90:941–9.
611 https://doi.org/10.1007/s11746-013-2243-y

612 (16) Cholakova D, Tcholakova S, Denkov N. Polymorphic phase transitions in bulk triglyceride
613 mixture. Cryst Growth Des. 2023;23: 2075–91. https://doi.org/10.1021/acs.cgd.2c01021

614 (17) Craven RJ, Lencki RW. Polymorphism of acylglycerols: a stereochemical perspective. Chem
615 Rev. 2013;113:7402–20. https://doi.org/10.1021/cr400212r

616 (18) Douaire M, di Bari V, Norton JE, Sullo A, Lillford P, Norton IT. Fat crystallisation at oil-
617 water interfaces. Adv Colloid Interface Sci. 2014;203:1–10.
618 https://doi.org/10.1021/acs.cgd.2c01021

619 (19) Engström L. Triglyceride systems forming molecular compounds. Fat Sci Dent Tech.
620 1992;94:173–81. https://doi.org/10.1002/lipi. 19920940503

621 (20) Floeter E, Haeupler M, Sato K. Molecular interactions and mixing phase behavior of lipid
622 crystals. In: Sato K, editor. Crystallization of lipids. Fundamentals and applications in food,

623 cosmetics and pharmaceuticals. Hoboken, NJ, USA: Wiley-Blackwell; 2018. p. 61–104.
624 https://doi.org/10.1002/9781118593882.ch3

625 (21) Ghazani SM, Marangoni AG. The ternary solid state phase behavior of triclinic POP, POS and
626 SOS and its relationship to CB and CBE properties. Cryst Growth Des. 2019a;19:704–13.
627 https://doi.org/10.1021/acs.cgd.8b01273

628 (21) Ghazani SM, Marangoni AG. The triclinic polymorphism of cocoa butter is dictated by its
629 major molecular species, 1-palmitoyl, 2-oleoyl, 3-stearoyl glycerol (POS). Cryst Growth Des.
630 2019b; 19:90–7. https://doi.org/10.1021/acs.cgd.8b00973

631 (22) Gibon V, Danthine S. Systematic investigation of co-crystallization properties in binary and
632 ternary mixtures of triacylglycerols containing palmitic and oleic acids in relation with palm
633 oil dry fractionation. Foods. 2020;9:1891. https://doi.org/10.3390/foods9121891

634 (22) Gibon V, Durant F, Deroanne C. Polymorphism and intersolubility of some palmitic, stearic
635 and oleic triglycerides: PPP, PSP and POP. J Am Oil Chem Soc. 1986;63:1047–55.
636 https://doi.org/10.1007/BF02673796

637 (23) Gresti J, Bugaut M, Maniongui C, Bezard J. Composition of molecular species of
638 triacylglcyerols in bovine milk fat. J Dairy Sci. 1993;76: 1850–69.
639 https://doi.org/10.3168/jds.S0022-0302(93)77518-9

640 (24) Hartel RW. Crystallization in foods. Gaithersburg, Maryland: Aspen Publishers Inc; 2001.

641 (25) Herrera ML, Hartel RW. Effect of processing conditions on crystallization kinetics of a milk
642 fat model system. J Am Oil Chem Soc. 2000;77:1177–88. https://doi.org/10.1007/s11746-
643 000-0184-4

644 (26) Ikeda E, Ueno S, Miyamoto R, Sato K. Phase behavior of a binary mixture of 1,3-dipalmitoyl-
645 2-oleoyl-sn-glycerol and 1,3-dioleoyl-2-palmitoyl-sn-glycerol in n-dodecane solution. J Phys
646 Chem B. 2010;114:10961–9. https://doi.org/10.1021/jp101821c

647 (27) Ikeda-Naito E, Hondoh H, Ueno S, Sato K. Mixing phase behavior of 1,3-dipalmitoyl-2-
648 oleoyl-snglycerol (POP) and 1,2-dipalmitoyl-3-oleoyl-rac-glycerol (PPO) in n-dodecane
649 solution. J Am Oil Chem Soc. 2014;91:1837–48. https://doi.org/10.1007/s11746-014-2534-y

650 (28) Joshi BL, Zielbauer BI, Vilgis TA. Comparative study on mixing behavior of binary mixtures
651 of cocoa butter/tristearin (CB/TS) and cocoa butter/coconut oil (CB/CO). Foods. 2020;9:327.
652 https://doi.org/10.3390/foods9030327

653 (29) Kaneko F, Kobayashi M, Sato K, Suzuki M. Martensitic phase transition of petroselinic acid:
654 influence of polytypic structure. J Phys Chem B. 1997;101:285–92.

655 https://doi.org/10.1021/jp9625927

656 (30) Koizumi H, Takagi M, Hondoh H, Michikawa S, Hirai Y, Ueno S. Control of phase separation
657 for CBS-based compound chocolates focusing on growth kinetics. Cryst Growth Des.
658 2022;22:6879–85. https://doi.org/10.1021/acs.cgd.2c00317

659 (31) Koyano T, Hachiya I, Sato K. Phase behavior of mixed systems of SOS and OSO. J Phys
660 Chem. 1992;96:10514–20. https://doi.org/10.1021/j100204a072

661 (32) Koyano T, Kato Y, Hachiya I, Unemura R. Crystallization behavior of ternary mixture of
662 POP/POS/SOS. J Japan Oil Chem Soc. 1993; 42:453–7.
663 https://doi.org/10.5650/jos1956.42.453

664 (33) Larsson K, Quinn P, Sato K, Tiberg F. Lipids: structure, physical properties and functionality.
665 Bridgwater, U.K.: Oily Press; 2006.

666 (34) Laustsen K. The nature of fat bloom in molded compound coatings. The Manufacturing
667 Confectioner. Princeton, WI: MC Publishing Company; Volume 71; 1991. p. 137–44.

668 (35) Lee J, Ye Y, Martini S. Physicochemical and oxidative changes in sonicated interesterified
669 soybean oil. J Am Oil Chem Soc. 2015; 92:305–8. https://doi.org/10.1007/s11746-014-2585-
670 0

671 (36) Lu C, Zhang B, Zhang H, Guo Y, Dang L, Liu Z, et al. Solid–liquid phase equilibrium and
672 phase behaviors for binary mixtures composed of tripalmitoylglycerol (PPP), 1,3-dipalmitoyl-
673 2-oleoylglycerol (POP), and 1,2-dioleoyl-3-palmitoyl-glycerol (POO). Ind Eng Chem Res.
674 2019;58:10044–52. https://doi.org/10.1021/acs.iecr.9b01947

675 (37) Lusi M. A rough guide to molecular solid solution: design, synthesis and characterization of
676 mixed crystals. Cryst Eng Commun. 2018;20:7042–52. https://doi.org/10.1039/C8CE00691A

677 (38) Macridachis J, Bayés-García L, Calvet T. An insight into the solidstate miscibility of
678 triacylglycerol crystals. Molecules. 2020;25: 4562.
679 https://doi.org/10.3390/molecules25194562

680 (39) Macridachis J, Bayés-García L, Calvet T. Mixing phase behavior of tripalmitin and oleic-rich
681 molecular compound-forming triacylglycerols. Ind Eng Chem Res. 2021;60:5374–84.
682 https://doi.org/10.1021/acs.iecr.1c00324

683 (40) Macridachis J, Bayés-García L, Calvet T. Solid phase behavior of mixture systems based on
684 tripalmitoyl glycerol and monounsaturated triacylglycerols forming a molecular compound.
685 Phys Chem Chem Phys. 2022;24:3749–60. https://doi.org/10.1039/D1CP05361B

686 (41) Mahisanunt B, Hondoh H, Ueno S. Coconut oil crystallization on tripalmitin and tristearin

seed crystals with different polymorphs. Cryst Growth Des. 2021;20:4980–90. https://doi.org/10.1021/acs.cgd.0c00064

(42) Mao J, Gao Y, Meng Z. Crystallization and phase behavior in mixture systems of anhydrous milk fat, palm stearin, and palm oil: formation of eutectic crystals. Food Chem. 2023;399:133877. https://doi.org/10.1016/j.foodchem.2022.133877

(43) Martini S. Sonocrystallization of fats. Springer Briefs in Food, Health, and Nutrition. New York, NY: Springer; 2013. https://doi.org/10.1007/978-1-4614-7693-1_6

(44) Mazzanti G, Li M, Marangoni AG, Idziak SHJ. Effects of shear rate variation on the nanostructure of crystallizing triglycerides. Cryst Growth Des. 2011;11:4544–50. https://doi.org/10.1021/cg200786k

(45) Minato A, Ueno S, Smith K, Amemiya Y, Sato K. Thermodynamic and kinetic study on phase behavior of binary mixtures of POP and PPO forming molecular compound systems. J Phys Chem B. 1997;101:3498–505. https://doi.org/10.1021/jp962956v

(46) Minato A, Ueno S, Yano J, Smith K, Seto H, Amemiya Y, et al. Thermal and structural properties of sn-1,3-dipalmitoyl-2-oleoylglycerol and sn-1,3-dioleoyl-2-palmitoylglycerol binary mixtures examined with synchrotron radiation X-ray diffraction. J Am Oil Chem Soc. 1997;74:1213–20. https://doi.org/10.1007/s11746-997-0047-7

(47) Minato A, Ueno S, Yano J, Wang ZH, Seto H, Amemiya Y, et al. Synchrotron radiation X-ray diffractions study on phase behavior of PPP-POP binary mixtures. J Am Oil Chem Soc. 1996;73:1567–72. https://doi.org/10.1007/BF02523526

(48) Minato A, Yano J, Ueno S, Smith K, Sato K. FT-IR study on microscopic structures and conformations of POP-PPO and POPOPO molecular compounds. Chem Phys Lipids. 1997;88:63–71. https://doi.org/10.1016/S0009-3084(97)00045-5

(49) Mizobe H, Tanaka T, Hatakeyama N, Nagai T, Ichioka K, Hondoh H, et al. Structures and binary mixing characteristics of enantiomers of 1-oleoyl-2,3-dipalmitoyl-sn-glycerol (S-OPP) and 1,2-dipalmitoyl-3-oleoyl-sn-glycerol (R-PPO). J Am Oil Chem Soc. 2013;90:1809–17. https://doi.org/10.1007/s11746-013-2339-4

(50) Myher JJ, Kuksis A, Marai L, Sandra P. Identification of the more complex triacylglycerols in bovine milk fat by gas chromatography-mass spectrometry using polar capillary columns. J Chromatogr. 1988;452:93–118. https://doi.org/10.1016/S0021-9673(01)81440-0

(51) Mykhaylyk OO, Smith KW, Martin CM, Ryan AJ. Structural models of metastable phases occurring during the crystallization process of saturated/unsaturated triacylglycerols. J Appl Cryst. 2007;40: 297–302. https://doi.org/10.1107/S0021889806055191

(52) Nakanishi K, Mikiya Y, Ishiguro T, Ueno S. Crystallization behavior of molecular compound in binary mixture system of 1,3-dioleoyl-2-palmitoyl-sn-glycerol and 1,3-dipalmitoyl-2-oleoyl-sn-glycerol. J Am Oil Chem Soc. 2018;95:51–9. https://doi.org/10.1002/aocs.12005

(53) Povey MJW. Crystal nucleation in food colloids. Food Hydrocoll. 2014;42:118–29. https://doi.org/10.1016/j.foodhyd.2014.01.016

(54) Rincón-Cardona JA, Agudelo-Laverde LM, Herrera ML, Martini S. Effect of high-intensity ultrasound on the crystallization behavior of high-stearic high-oleic sunflower oil soft stearin. J Am Oil Chem Soc. 2015;92:473–82. https://doi.org/10.1007/s11746-015-2620-9

(55) Rossell JB. Fractionation of lauric oils. J Am Oil Chem Soc. 1985;62: 385–90. https://doi.org/10.1007/BF02541409

(56) Rousset P, Rappaz M, Minner E. Polymorphism and solidification kinetics of the binary system POS/SOS. J Am Oil Chem Soc. 1998;75:857–64. https://doi.org/doi:10.1007/s11746-998-0237-y

(57) Sasaki M, Ueno S, Sato K. Polymorphism and mixing phase behavior of major triacylglycerols of cocoa butter. In: Garti N, Widlak NR, editors. Cocoa butter and related compounds. Urbana, IL, USA: AOCS Press; 2012. p. 151–72. https://doi.org/10.1016/B978-0-9830791-2-5.50009-8

(58) Seilert J, Moorthy AS, Kearsley AJ, Floeter E. Revisiting a model to predict pure triglyceride properties: parameter optimization and performance. J Am Oil Chem Soc. 2021;98:837–50. https://doi.org/10.1002/aocs.12515

(59) Sibbald AN, Carney JR, Marangoni AG. Enhanced structuring of fat with reduced saturates using mixed molecular compounds. J Am Oil Chem Soc. 2016;93:1441–52. https://doi.org/10.1007/s11746-015-2718-0

(60) Smith KW. Confectionery fats. In: Garti N, Widlak NR, editors. Cocoa butter and related compounds. Urbana, IL, USA: AOCS Press; 2012. p. 475–95. https://doi.org/10.1016/B978-0-9830791-2-5. 50022-0

(61) Smith KW, Bhaggan K, Talbot G, van Malssen K. Crystallization of lipids: influence of minor components and additives. J Am Oil Chem Soc. 2011;88:1085–101. https://doi.org/10.1007/s11746-011-1819-7

(62) Sonwai S, Mackley MR. The effect of shear on the crystallization of cocoa butter. J Am Oil Chem Soc. 2006;83:583–96. https://doi.org/10.1007/s11746-006-1243-6

(63) Takeuchi M, Ueno S, Sato K. Crystallization kinetics of polymorphic forms of a molecular

compound constructed by SOS (1,3-distearoyl-2-oleoyl-sn-glycerol) and SSO (1,2-distearoyl-3-oleoyl-rac-glycerol). Food Res Int. 2002;35:919–26. https://doi.org/10.1016/S0963-9969(02)00154-0

(64) Talbot G. Properties of cocoa butter and vegetable fats. In: Beckett ST, Fowler MS, Ziegler GR, editors. Beckett's industrial chocolate manufacture and use. 5th ed. Chichester: Wiley-Blackwell; 2017. p. 153–84. https://doi.org/10.1002/9781118923597.ch7

(65) Timms RE. Phase behaviour of fats and their mixtures. Prog Lipid Res. 1984;23:1–38. https://doi.org/10.1016/0163-7827(84)90004-3

(66) Timms RE. Chapter 6 – Production and characteristic properties. Confectionery fats handbook. Cambridge: Woodhead Publishing Limited; 2003. p. 191–254.

(67) Watanabe S, Yoshikawa S, Arishima T, Sato K. Polymorphism and mixing phase behavior in ternary mixture systems of SOS-SSOOSO: formation of molecular compound crystals. J Am Oil Chem Soc. 2018;95:447–60. https://doi.org/10.1002/aocs.12054

(68) Watanabe S, Yoshikawa S, Sato K. Formation and properties of dark chocolate prepared using fat mixtures of cocoa butter and symmetric/asymmetric stearic-oleic mixed-acid triacylglycerols: impact of molecular compound crystals. Food Chem. 2021;339: 127808. https://doi.org/10.1016/j.foodchem.2020.127808

(69) Watanabe S, Yoshikawa S, Sato K. Physical properties and fat bloom stability of compound chocolates made with ternary fat blends of cocoa butter, 1,3-dioleoyl-2-stearoyl-triacylglycerol-fat, and lauric-based cocoa butter substitute. J Oleo Sci. 2023;72:1073–1082. https://doi.org/10.5650/jos.ess23159

(70) Wesdorp LH, van Meeteren J, de Jon S, Giessen R, Overbosch P, Grootscholten P. Liquid-multiple solid phase equilibria in fats: theory and experiments. In: Marangoni AG, Wesdorp LH, editors. Structure and properties of fat crystal networks. Volume 2. 2nd ed. Boca Raton: CRC Press; 2013. p. 241–418. https://doi.org/10.1201/b12883

(71) Wijarnprecha K, West R, Rousseau D. Temperature-dependent mixing behavior of tristearin and 1,2-distearoyl-3-oleoyl-rac-glycerol (SSO). Cryst Growth Des. 2023;23:4807–14. https://doi.org/10.1021/acs.cgd.2c01514

(72) Ye Y, Tan CY, Kim DA, Martini S. Application of high-intensity ultrasound to a zero-trans shortening during temperature cycling at different cooling rates. J Am Oil Chem Soc. 2014;91:1155–69. https://doi.org/10.1007/s11746-014-2458-6

(73) Yoshikawa S, Kida H, Sato K. Promotional effects of new types of additives on lipid crystallization. J Oleo Sci. 2014;63:333–45. https://doi.org/10.5650/jos.ess13155

(74) Yoshikawa S, Watanabe S, Yamamoto Y, Kaneko F, Sato K. Interactive polymorphic crystallization behavior in eutectic triacylglycerol mixtures containing molecular compound crystals. Cryst Growth Des. 2022;22:1753–63. https://doi.org/10.1021/acs.cgd.1c01340

(79) Zhang L, Ueno S, Miura S, Sato K. Binary phase behavior of 1,3-dipalmitoyl-2-oleoyl-sn-glycerol and 1,2-dioleoyl-3-palmitoylracglycerol. J Am Oil Chem Soc. 2007;84:219–27. https://doi.org/10.1007/s11746-006-1034-0

(80) Zhang L, Ueno S, Sato K. Binary phase behavior of saturatedunsaturated mixed-acid triacylglycerols – a review. J Oleo Sci. 2018;67:679–87. https://doi.org/10.5650/jos.ess17263

(81) Zhang L, Ueno S, Sato K, Adlof RO, List GR. Thermal and structural properties of binary mixtures of 1,3-distearoyl-2-oleoyl-glycerol (SOS) and 1,2-dioleoyl-3-stearoyl-sn-glycerol (sn-OOS). J Therm Anal Calorim. 2009;98:105–11. https://doi.org/10.1007/s10973-009-0451-3

(82) Zhang L, Wei KJ, Chen JC, Xiong M, Li X, Hondoh H, et al. Effect of cis–trans isomerization on the crystallization behavior of triacylglycerols. Cryst Growth Des. 2020;20:1655–64. https://doi.org/10.1021/acs.cgd.9b01406

Table 1. Relative concentrations (%) of CBS, CB, and OSO-fat in total chocolate fat in eight chocolate samples.

Sample	CBS	OSO-fat	CB
A1	90.0	0.0	10.0
A2	85.0	0.0	15.0
A3	80.0	0.0	20.0
A4	75.0	0.0	25.0
B1	80.0	10.0	10.0
B2	70.0	15.0	15.0
B3	60.0	20.0	20.0
B4	50.0	25.0	25.0

Table 2. Evaluation of fat bloom formation of eight dark chocolate samples after storage for 3 weeks (3 W) and 15 weeks (15 W) under different thermal conditions, -; no fat bloom, +; slightly bloomed, ++; fairly bloomed, +++: seriously bloomed.

	15°C		20°C		25°C		15–25°C	
Chocolate sample	3 W	15 W	3 W	15 W	3 W	15 W	3 W	15 W
A1	+	+++	+	++	–	++	–	+
A2	+	+++	+	++	–	++	–	+
A3	+	+++	+	++	+	++	–	+
A4	+	+++	+	++	+	++	–	+
B1	–	–	–	–	–	–	–	–
B2	–	–	–	–	–	–	–	–
B3	–	–	–	–	–	–	–	–
B4	–	–	–	–	–	–	–	–

Figures Captions

Figure 1. Typical three binary mixing systems of triacylglycerols (TAGs). (a) and (b): component TAGs, L; liquid phase, S_A, S_B, and S_{MC}; solid phases of A, B and molecular compound (MC).

Figure. 2. Combination of saturated (S_{at})-unsaturated (U) mixed-acid TAGs exhibiting MC-forming and eutectic binary mixtures.

Figure 3. Key factors affecting the formation of MC crystals in binary mixtures of TAGs containing palmitic (P) and oleic (O) acid moiety. Three problems in MC crystal formation of the double chain-length structure are indicated in $MC_{POP/OPO}$ model: the chain packing between P and O chains by dashed boxes, stacking of glycerol groups by a dotted oval box, and π–π interactions between cis-double bonds of the oleic acid chains by an arrow.

Figure 4. Mixing phase behavior of PEP and EPE. Source: Reprinted with permission from Lu Zhang et al., 2020. Copyright 2020 American Chemical Society.

Figure 5. DSC thermogram and SR-XRD patterns of PEP/EPE at a 50:50 ratio. Source: Reprinted with permission from Lu Zhang et al., 2020. Copyright 2020 American Chemical Society.

Figure 6. Postulated configuration of the molecular packing of EPE, PEP, and $MC_{PEP/EPE}$. The arrow indicates the void at the methyl end of PEP in β' form due to the chain length mismatch, which is filled by the acyl chain of EPE in $MC_{PEP/EPE}$, as indicated by the dotted lines. Source: Reprinted with permission from Lu Zhang et al., 2020. Copyright 2020 American Chemical Society.

Figure 7. Summary of temperature-dependent polymorphic crystallization in the binary mixtures of POP/OPO, POP/rac-PPO and POP/sn-PPO. Source: Reprinted with permission from Bayés-García et al., 2023. Copyright 2023 American Chemical Society.

Figure 8. Effects of chain packing and glycerol conformation on the formation of MC crystals. Source: Reprinted with permission from Bayés-García et al., 2023. Copyright 2023 American Chemical Society.

Figure 9. Phase behavior of LLL/SOS/OSO mixtures with different weight fractions of SOS/OSO = 1/1 (WSOS/OSO): melting of MCSOS/OSO β -2 (□), transformation β_2-2 → β_1-2 of LLL (▲), and melting of LLL β_1-2 (●). Source: Reprinted with permission from Yoshikawa et al., 2022. Copyright 2022 American Chemical Society.

Figure 10. 3D surface plots and overhead projections of SR-XRD data on LLL/SOS/OSO = 2/1/1 (a) and 1/2/2 (b), taken during cooling at a rate of 2°C/min, holding at 15°C for 30 min, and heating at a rate of 5°C/min. Numbers hyphenated to Greek letters for crystal polymorphs represent the chain-length structure. jsj is the magnitude of scattering vector ($|s| = 2\sin\theta/\lambda = 1/d$), where θ is the Bragg angle, λ is the x-ray wavelength applied, and d is the spacing between diffracting planes. Unit: nm.

868 **Figure 11**. 3D surface plots and overhead projections of SR-XRD data on LLL/SOS/rac-
869 SOO = 2/1/1, taken during cooling at a rate of 2°C/min, holding at 15°C for 30 min, and
870 heating at a rate of 5°C/min. Numbers hyphenated to Greek letters for crystal polymorphs
871 represent the chain-length structure. Unit: nm.

872 **Figure 12**. Phase diagram of ternary mixture systems of SOS/SSO/OSO. White symbols
873 represent MC crystals of β-2, black symbols represent eutectic mixtures of β-2 of MC
874 crystals and component TAG.

875 **Figure 13**. SFC profiles of CB and CB/SSO-fat/OSO-fat blends. Blending ratio of (a)–(f)
876 are as follows. CB/SSO-fat/OSO-fat = (a) 50/50/0, (b) 50/40/10, (c) 50/30/20, (d) 50/20/30,
877 (e) 50/10/40, and (f) 50/0/50.

878 **Figure 14**. XRD patterns of fat blends of (a) CBS/CB and (b) CBS/$MC_{CB/OSO}$ before (dot
879 line) and after (black line) 6 months storage at 20°C (unit: nm).

880

881

882

Figure 1

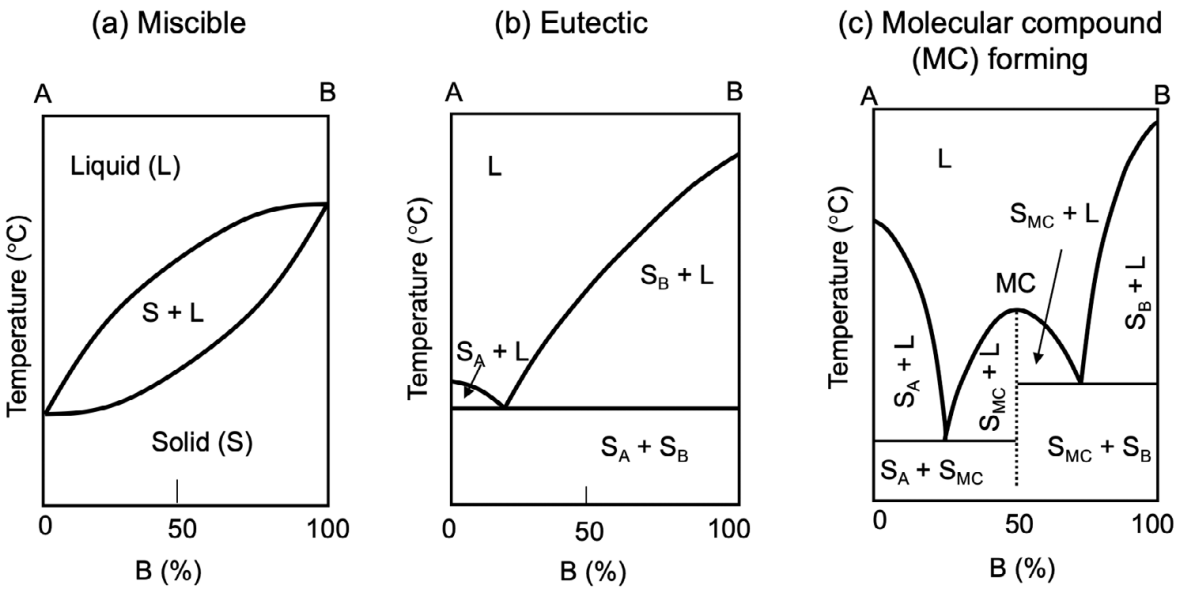
(a) Miscible
A
B
Liquid (L)
S + L
Solid (S)
Temperature (°C)
0
50
100
B (%)
(b) Eutectic
A
B
L
S_B + L
S_A + L
S_A + S_B
Temperature (°C)
0
50
100
B (%)
(c) Molecular compound (MC) forming
A
B
L
S_{MC} + L
MC
S_B + L
S_A + L
S_{MC} + L
S_A + S_{MC}
S_{MC} + S_B
Temperature (°C)
0
50
100
B (%)

Figure 2

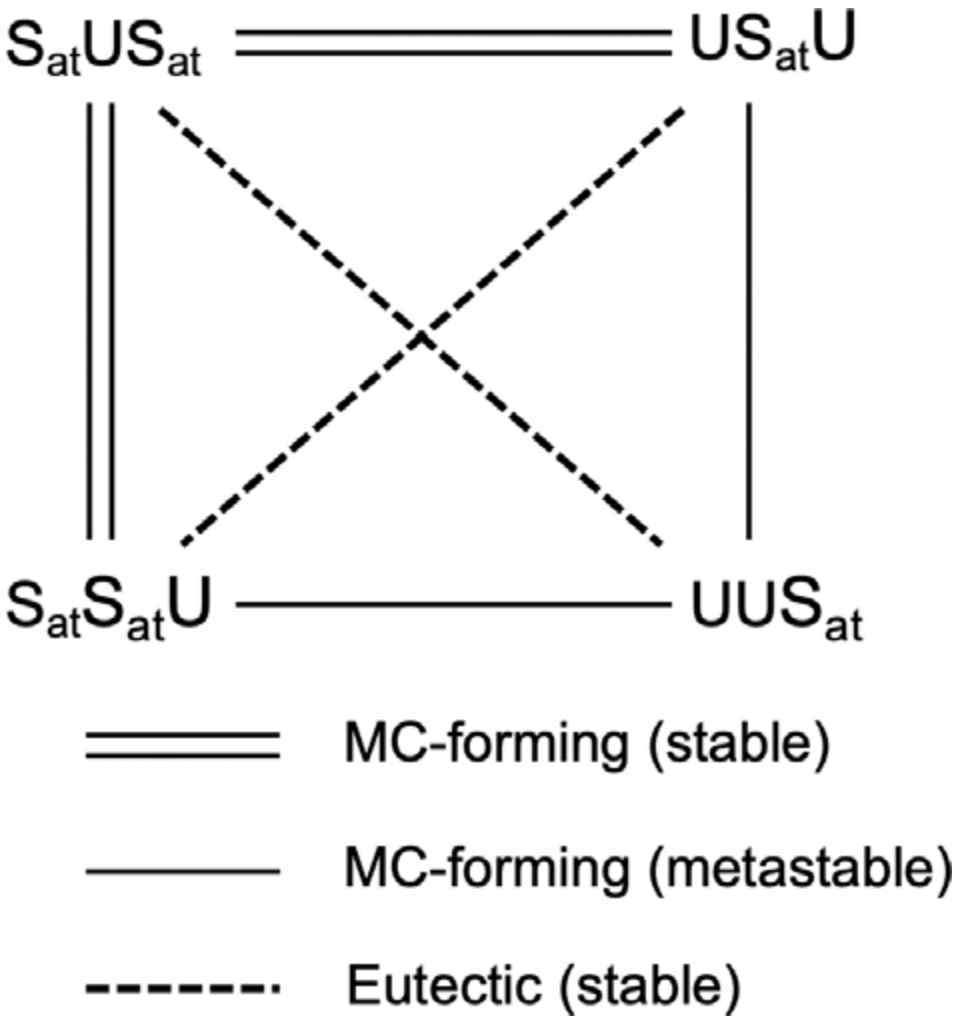
$S_{at}US_{at}$
$US_{at}U$
$S_{at}S_{at}U$
UUS_{at}
MC-forming (stable)
MC-forming (metastable)
Eutectic (stable)

Figure 3

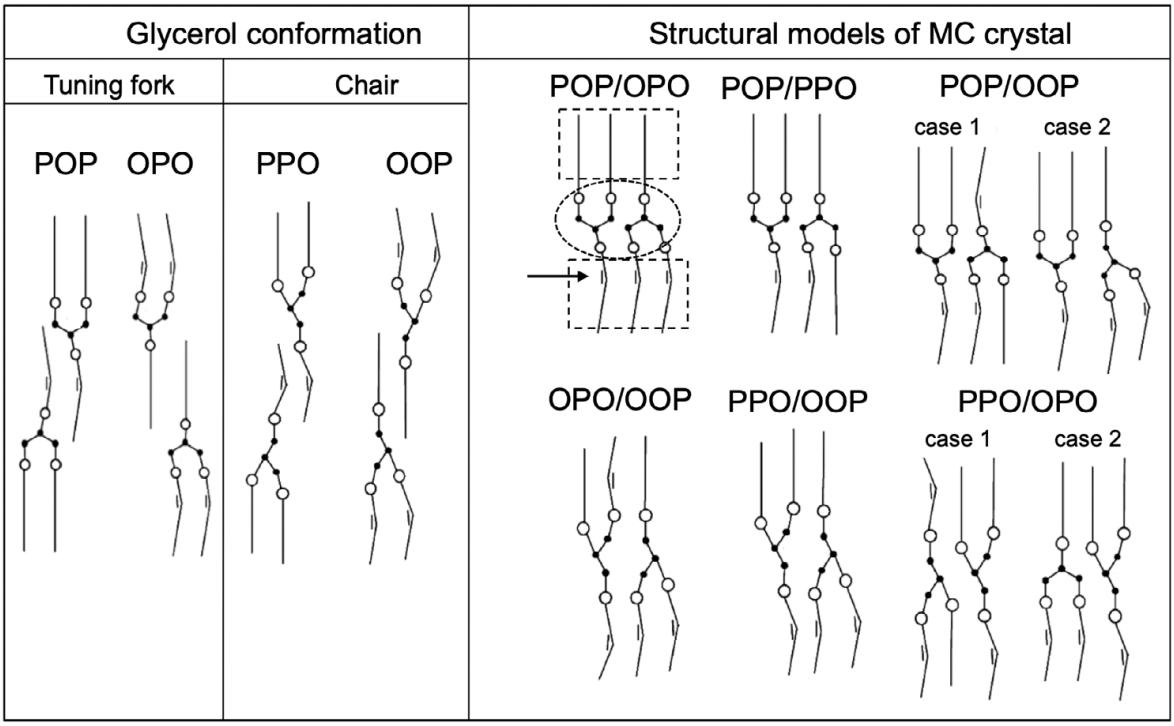
Glycerol conformation
Structural models of MC crystal
Tuning fork
Chair
POP
OPO
PPO
OOP
POP/OPO
POP/PPO
POP/OOP
case 1
case 2
OPO/OOP
PPO/OOP
PPO/OPO
case 1
case 2

Figure 4

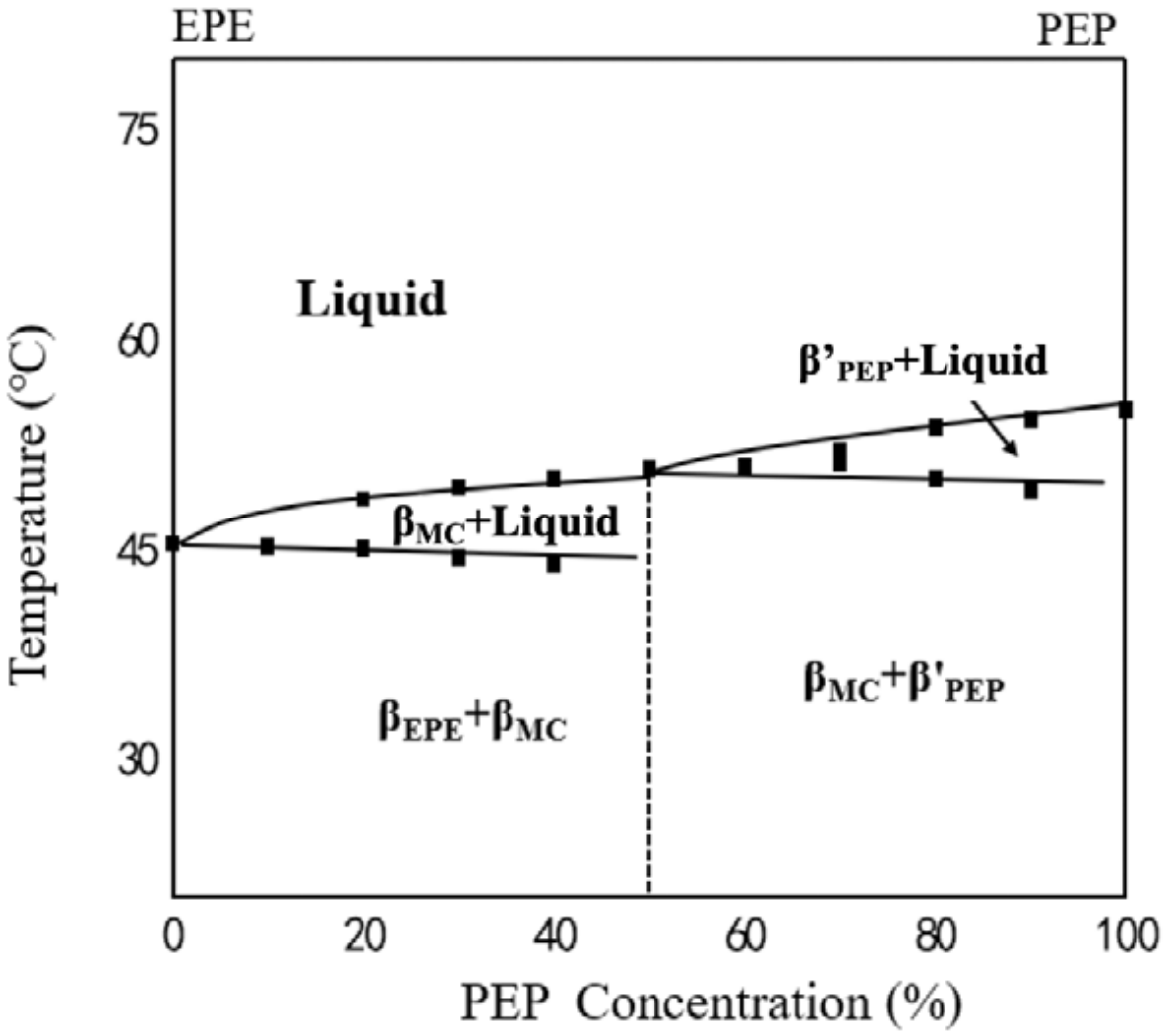
EPE
PEP
75
60
45
30
Liquid
β'PEP+Liquid
βMC+Liquid
βEPE+βMC
βMC+β'PEP
Temperature (°C)
0
20
40
60
80
100
PEP Concentration (%)

Figure 5

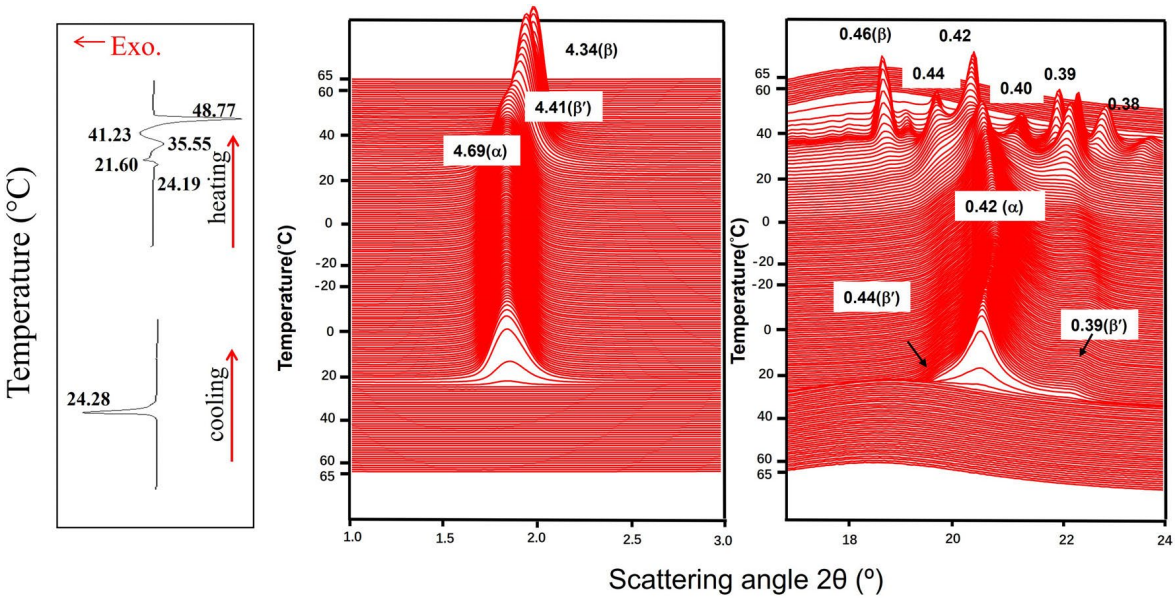
Exo.
48.77
41.23
35.55
21.60
24.19
heating
24.28
cooling
Temperature (°C)
4.34(β)
4.41(β′)
4.69(α)
Temperature(°C)
0.46(β)
0.42
0.44
0.40
0.39
0.38
0.42 (α)
0.44(β′)
0.39(β′)
Temperature(°C)
Scattering angle 2θ (°)

Figure 6

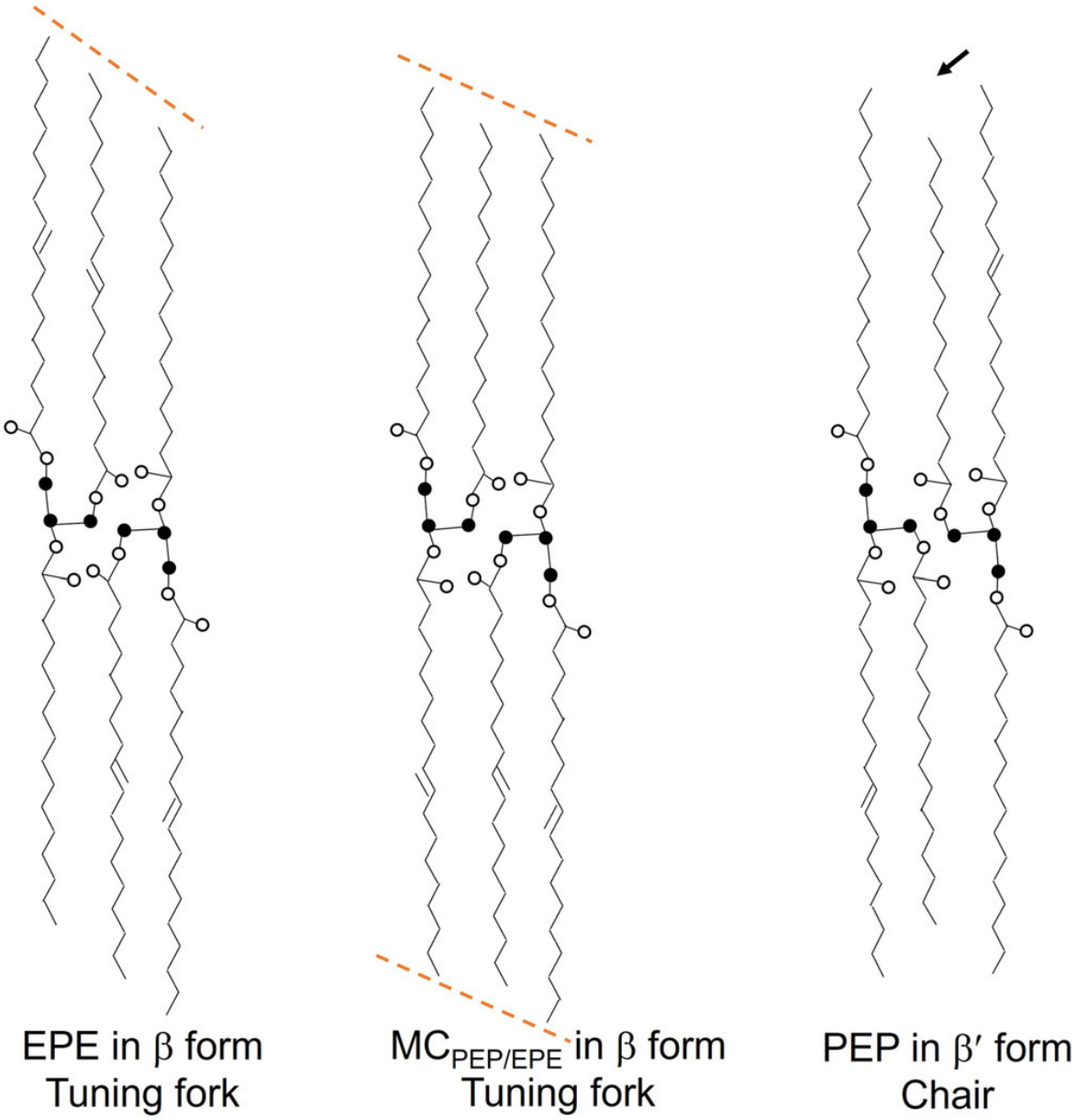
EPE in β form
Tuning fork
MC$_{PEP/EPE}$ in β form
Tuning fork
PEP in β′ form
Chair

Figure 7

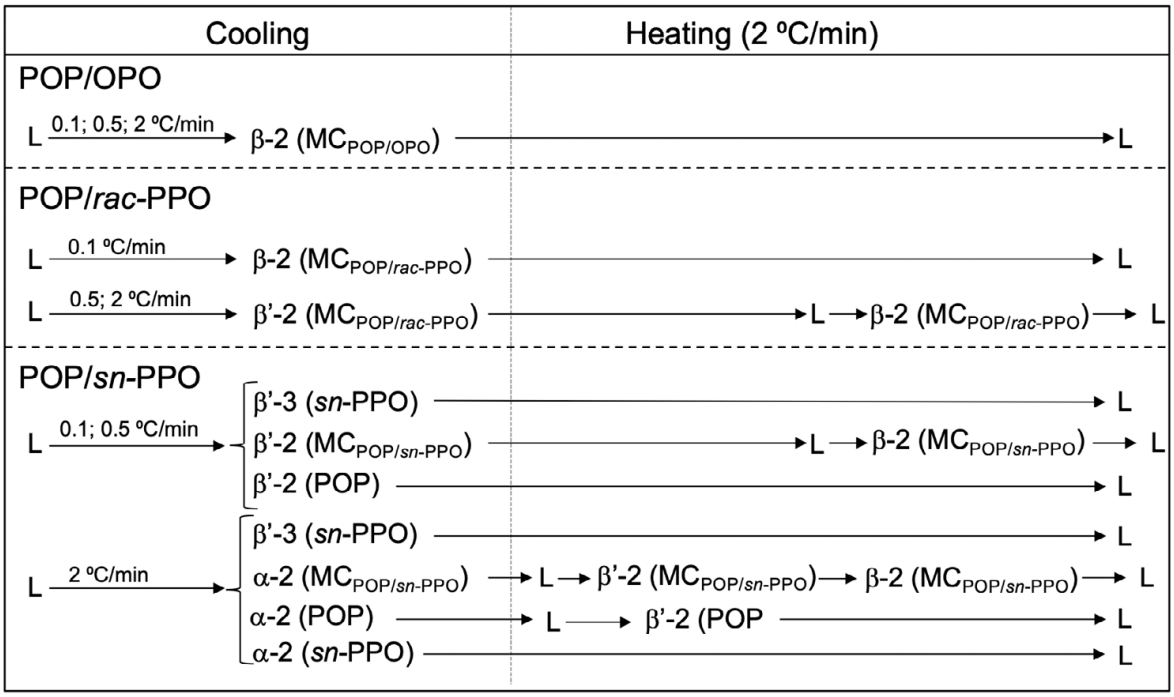
Cooling
Heating (2 ºC/min)
POP/OPO
L
0.1; 0.5; 2 ºC/min
β-2 (MC POP/OPO)
L
POP/rac-PPO
L
0.1 ºC/min
β-2 (MC POP/rac-PPO)
L
L
0.5; 2 ºC/min
β'-2 (MC POP/rac-PPO)
L
β-2 (MC POP/rac-PPO)
L
POP/sn-PPO
L
0.1; 0.5 ºC/min
β'-3 (sn-PPO)
L
β'-2 (MC POP/sn-PPO)
L
β-2 (MC POP/sn-PPO)
L
β'-2 (POP)
L
L
2 ºC/min
β'-3 (sn-PPO)
L
α-2 (MC POP/sn-PPO)
L
β'-2 (MC POP/sn-PPO)
β-2 (MC POP/sn-PPO)
L
α-2 (POP)
L
β'-2 (POP
L
α-2 (sn-PPO)
L

Figure 8

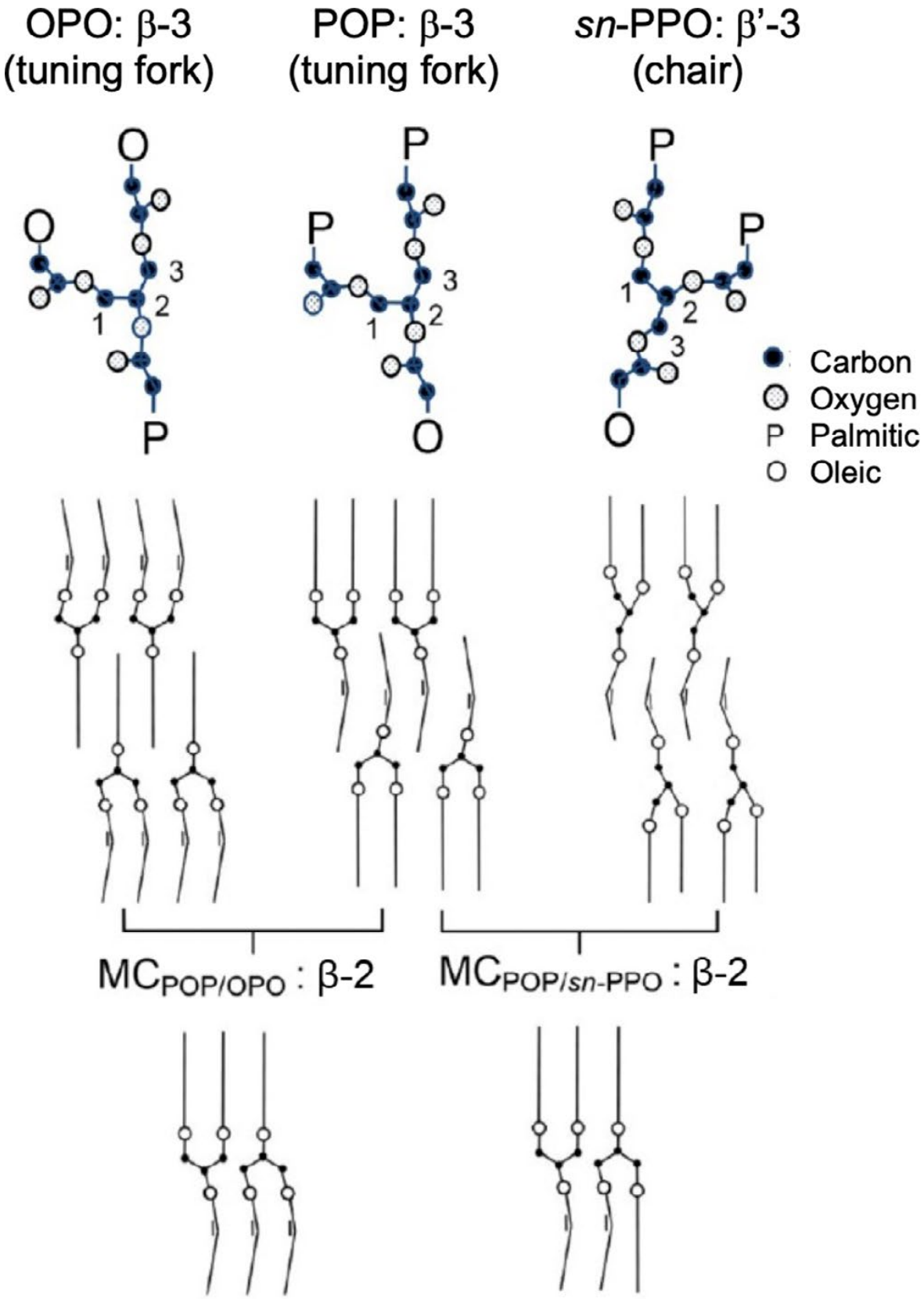
OPO: β-3
(tuning fork)
POP: β-3
(tuning fork)
sn-PPO: β'-3
(chair)
O
O
P
P
P
O
P
P
O
1
2
3
Carbon
Oxygen
P Palmitic
O Oleic
MC POP/OPO : β-2
MC POP/sn-PPO : β-2

948 **Figure 9**

949

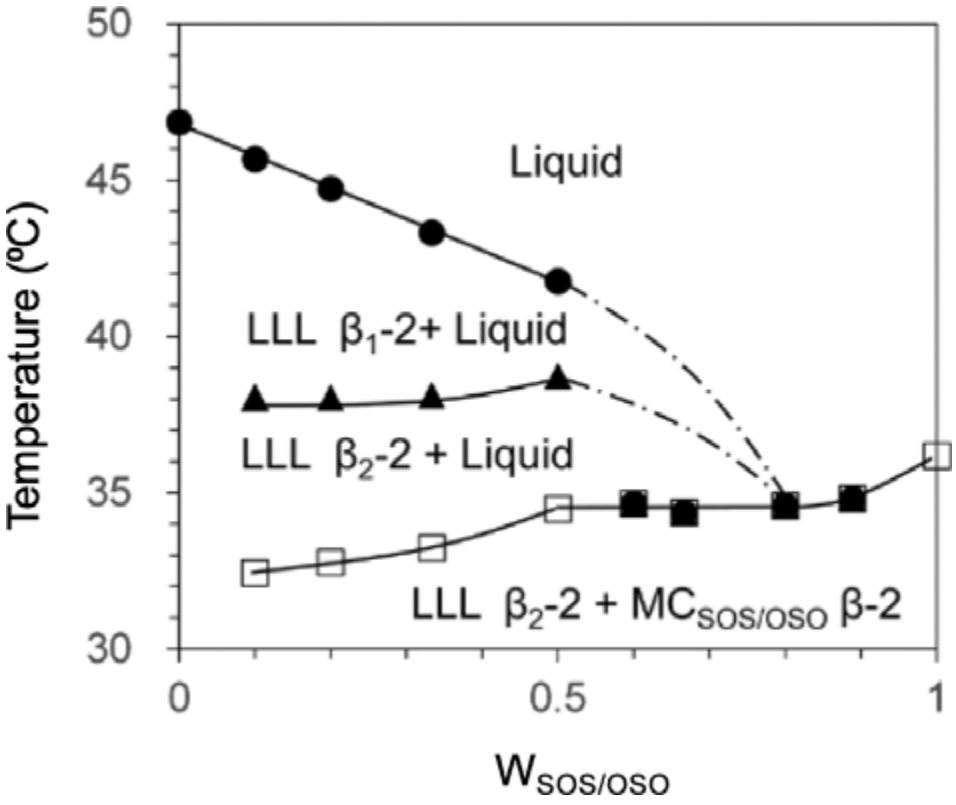

950

951

952

953

954

955

Figure 10

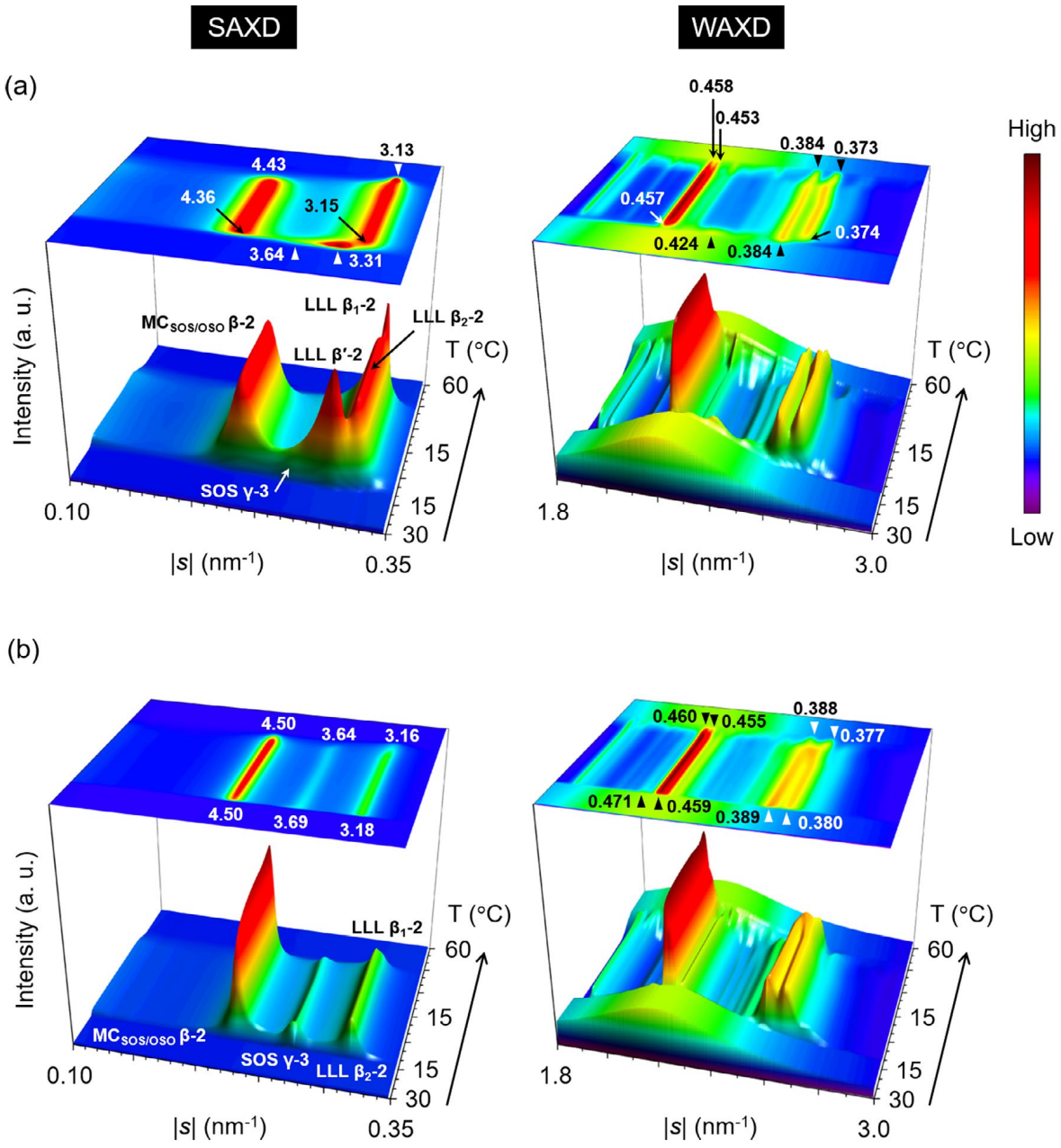
SAXD
WAXD
(a)
4.43
4.36
3.15
3.13
3.64
3.31
MC SOS/OSO β-2
LLL β1-2
LLL β2-2
LLL β'-2
SOS γ-3
Intensity (a. u.)
T (°C)
60
15
15
30
0.10
0.35
|s| (nm-1)
0.458
0.453
0.384
0.373
0.457
0.374
0.424
0.384
1.8
3.0
High
Low
(b)
4.50
3.64
3.16
4.50
3.69
3.18
LLL β1-2
MC SOS/OSO β-2
SOS γ-3
LLL β2-2
0.388
0.460
0.455
0.377
0.471
0.459
0.389
0.380

Figure 11

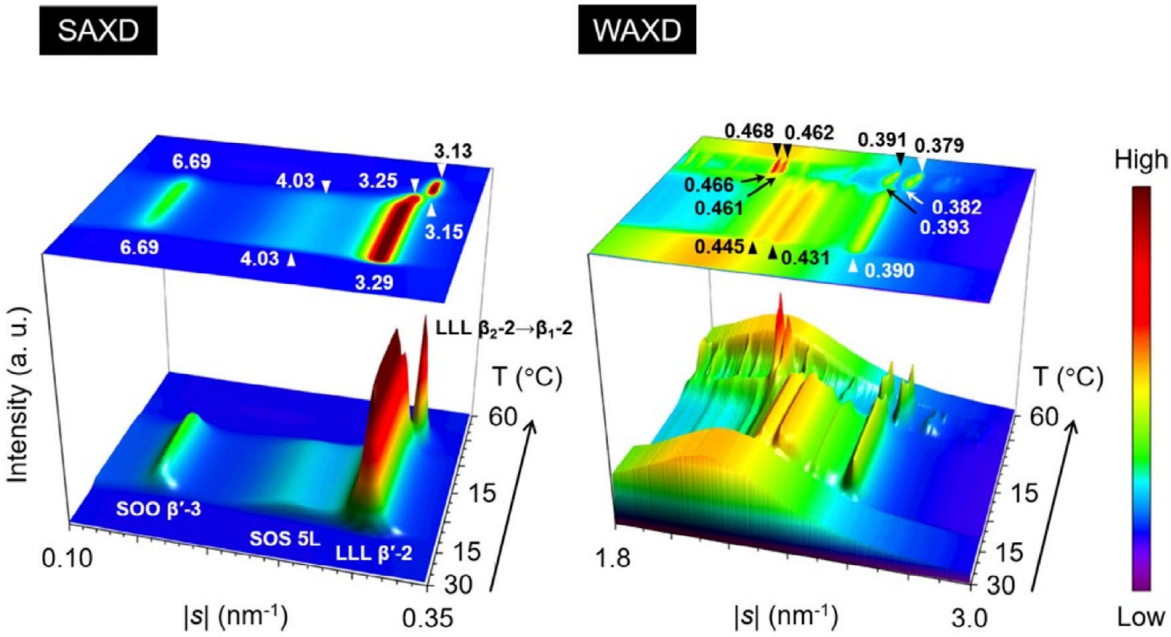
SAXD
WAXD
6.69
4.03
3.25
3.13
3.15
6.69
4.03
3.29
LLL β2-2→β1-2
Intensity (a. u.)
T (°C)
60
15
15
30
SOO β'-3
SOS 5L
LLL β'-2
0.10
|s| (nm-1)
0.35
0.468
0.462
0.391
0.379
0.466
0.461
0.382
0.393
0.445
0.431
0.390
High
Low
1.8
3.0

Figure 12

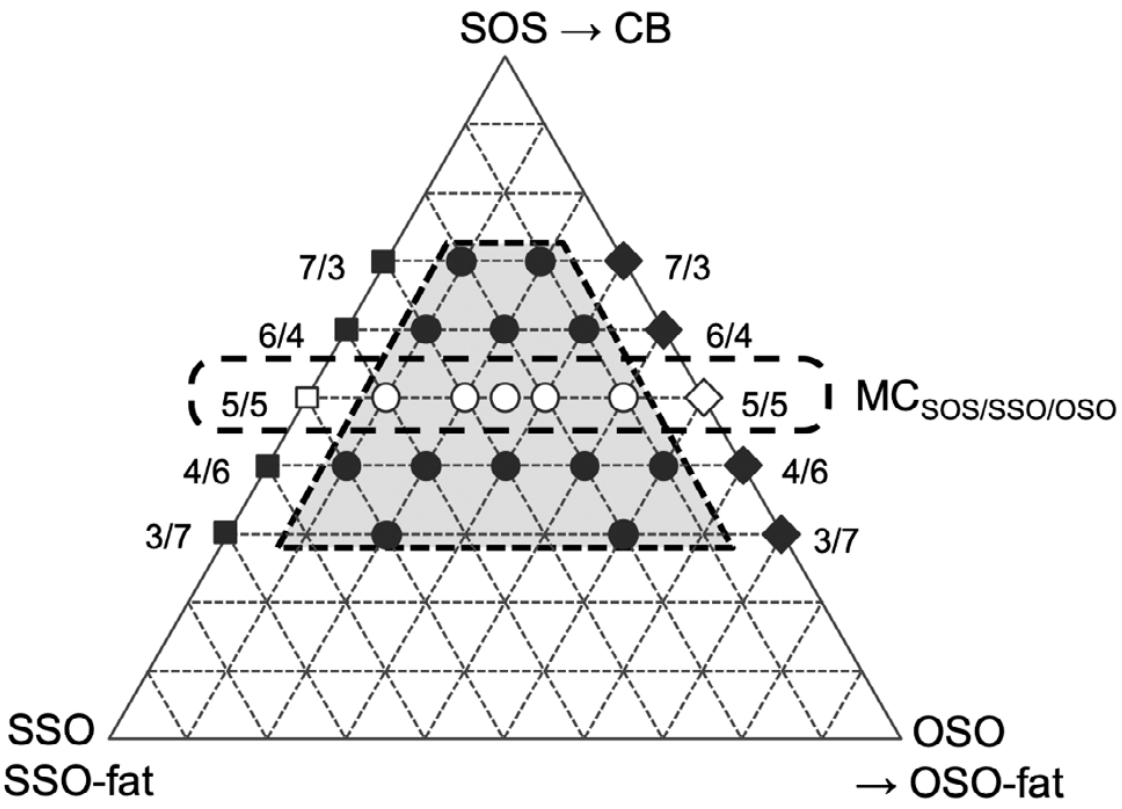
SOS → CB
7/3
7/3
6/4
6/4
5/5
5/5
MC SOS/SSO/OSO
4/6
4/6
3/7
3/7
SSO
→ SSO-fat
OSO
→ OSO-fat

Figure 13

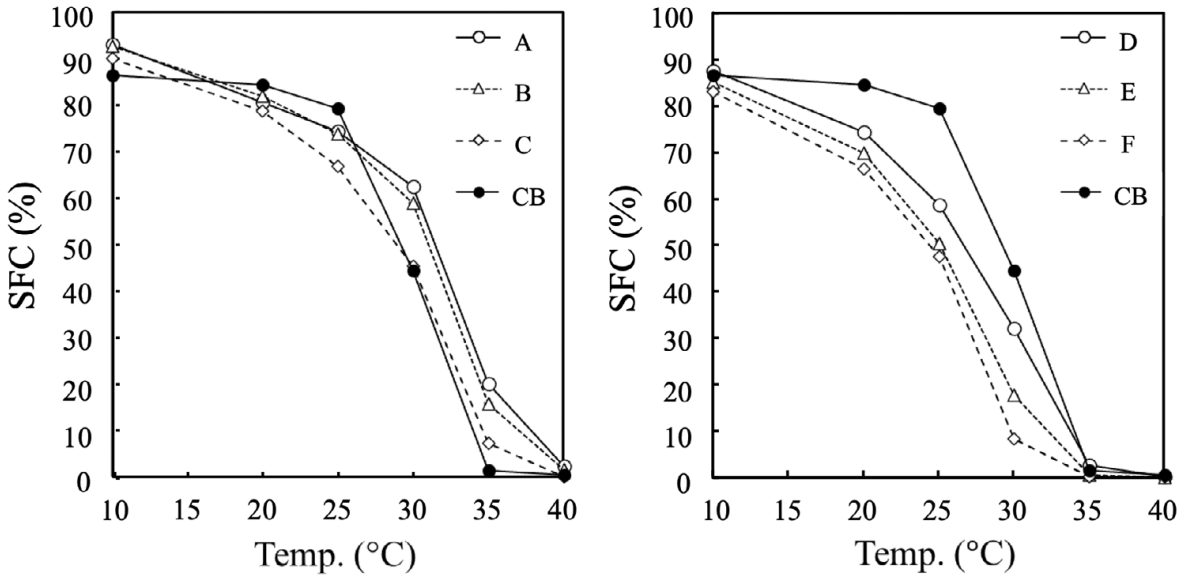

988 **Figure 14**

989

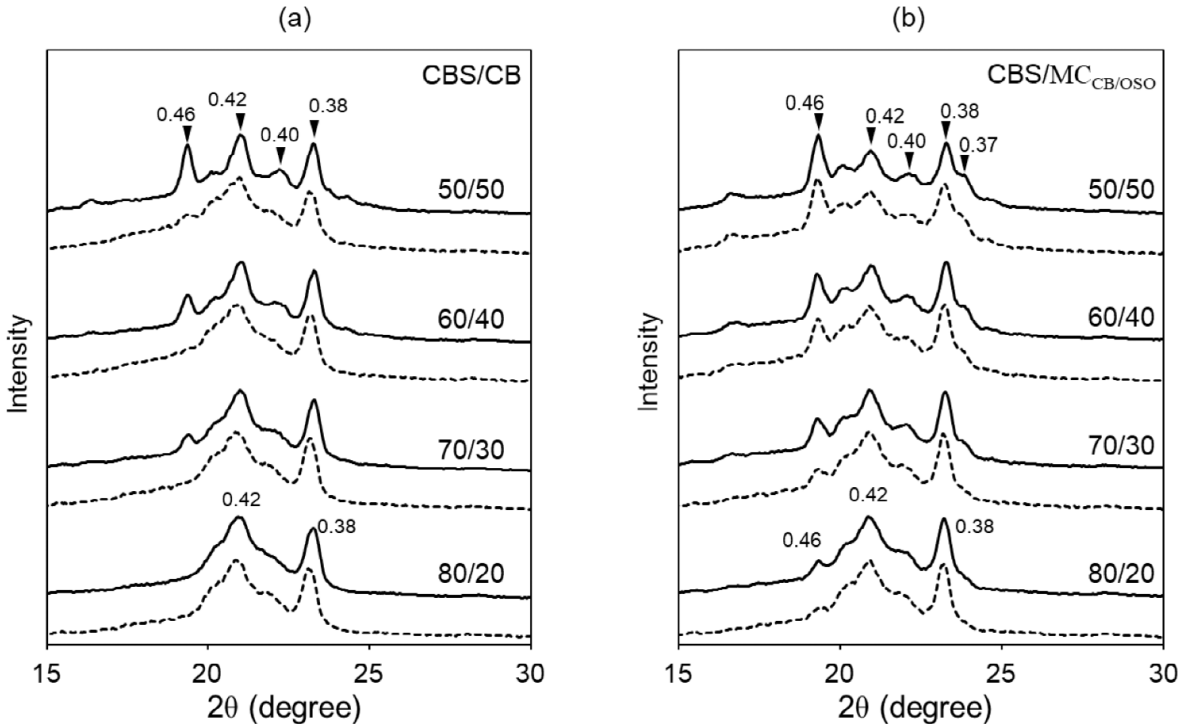

990

991

992

993